Chapter 6
Generalized Impact Laws and Multiple Impacts

We speak of a *multiple impact* when several collisions occur at the same time in a multibody system. Multiple impacts are complex phenomena which possess particular features, not shared by single impacts. In the first part of this chapter, these specific properties are described. Then, two models of multiple impacts are presented: the first one extends kinematic laws (Newton's and Moreau's impact laws), while the second one extends Darboux-Keller's impact dynamics and uses energetic coefficients of restitution at each contact/impact point. The extension of Poisson's kinetic law is briefly introduced. Chains of balls and the rocking block systems serve as examples.

6.1 Particular Features of Multiple Impacts

A multiple impact occurs each time several contact points of a system may undergo some (local) normal velocity jump ($v_{\mathrm{n},i}(t_k^+) \neq v_{\mathrm{n},i}(t_k^-)$, where i is the contacting points index). This encompasses those contacts with $v_{\mathrm{n},i}(t_k^-) = 0$, i.e. some contacts may be closed (or active) at the impact time, as is the case in the popular Newton's cradle where the balls touch each other at the shock instant (the same occurs for the rocking block system). More rigorously we may state the following. Consider an n-degree-of-freedom system with a configuration space $\mathscr{Q}$, subjected to m unilateral constraints $f(q) \geq 0$. The admissible domain is $\Phi = \{q \in \mathscr{Q} | f(q) \geq 0\}$, impacts occur on its boundary $\mathrm{bd}(\Phi)$. The boundary is made of hypersurfaces $\Sigma_l \stackrel{\Delta}{=} \bigcap_{i=1}^{l} \Sigma_i$, with $\Sigma_i \subseteq \{q \in \mathbb{R}^n | f_i(q) = 0\}$ which is a codimension one hypersurface (with some abuse we will say that Σ_i has also codimension one). Therefore, Σ_l has codimension $l \geq 1$. Physically, this means that l unilateral constraints boundaries are reached at the same time t_k, including situations where some of them become active (i.e. $f_i(q(t)) > 0$ in a left-neighborhood of t_k, and $v_{\mathrm{n},i}(t_k^-) = \nabla f_i(q(t_k))^T \dot{q}(t_k^-) < 0$) while others were already active (i.e. $f_j(q(t)) = 0$ in a left-neighborhood of t_k, and $v_{\mathrm{n},j}(t_k^-) = \nabla f_j(q(t_k))^T \dot{q}(t_k^-) = 0$). The subtlety here is that the previously-lasting

B. Brogliato, *Nonsmooth Mechanics*, Communications and Control Engineering,
DOI 10.1007/978-3-319-28664-8_6

contacts may satisfy $v_{\mathrm{n},j}(t_k^+) = \nabla f_j(q(t_k))^T \dot{q}(t_k^+) > 0$, and this is why they are part of the multiple impact phenomenon. We will see later that such "distance effects" are due to wave transmission through the multibody system.

Definition 6.1 (*Multiple Impact*) We say that an $l-$multiple impact occurs each time the attained boundary hypersurface Σ_l has codimension $l \geq 0$.

Remark 6.1 Physically, and taking into account contact deformations, collisions at different points of a system may be declared to be simultaneous when they overlap and thus may influence each other. In a perfect rigid body model limit, they occur at the same time.

6.1.1 Some Specific Features of Multiple Impacts

A typical case of a multiple impact is the collision of a chain of N aligned identical balls with a rigid ground, as shown in Fig. 6.1. When the impact occurs, the balls are all contacting each other and an $N-1$-impact occurs. The chain is submitted to gravity, and starts at a height h. The mass of a stainless steel bead used in the experiment is $m = 2.05 \times 10^{-3}$ kg. The Young modulus and Poisson ratio for stainless steel are $E = 21 \times 10^{10}$ N/m^2 and $\nu_s = 0.276$, respectively. Thus, the value of the contact stiffness, K_i, $i = 2, \ldots, N$ for sphere/sphere contact is 6.9716×10^9 N/m$^{3/2}$. For the contact between the bead and the wall made of stainless steel, the value of the contact stiffness K_1 for the sphere-plane contact is 9.858×10^9 N/m$^{3/2}$.

It is shown experimentally in [387] and numerically in [749] that the maximum contact force during the impact process, is almost independent of N, i.e. of the total mass of the chain. This is a rather counter-intuitive result. In Fig. 6.2a are depicted the contact forces felt at the ground during the shock, for a column of $N = 1, 2, \ldots, 8$ beads with fall height $h = 3.1$ mm (pre-impact velocity 0.246 m/s). In Fig. 6.2b are depicted the contact forces felt at the ground during the shock, for a column of $N = 5, 6, \ldots, 12$ beads with fall height $h = 5.1$ mm (pre-impact velocity 0.316 m/s). The restitution coefficient between the beads is $e_{\mathrm{n},s} = 0.96$, and the restitution coefficient between the last particle and the ground is $e_{\mathrm{n},p} = 0.92$. The numerical

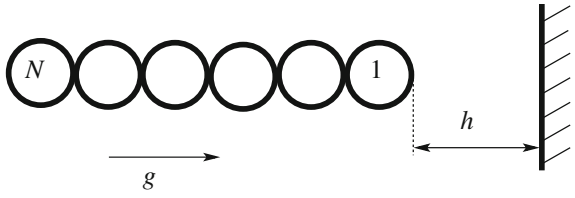

Fig. 6.1 A column of beads colliding against a wall

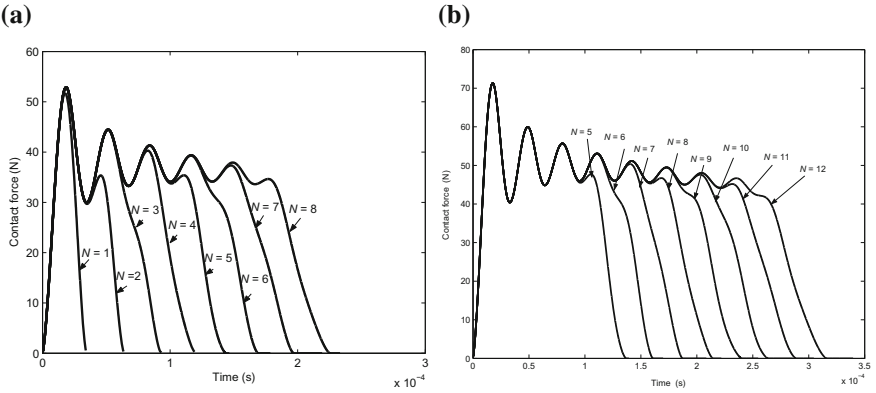

Fig. 6.2 The contact force at the wall during the collision. Taken from [749, Figs. 2, 3]. **a** $N = 1, \ldots, 8$. **b** $N = 5, \ldots, 12$

results are obtained with the LZB model, that is described in Sect. 6.3. Notice that the collisions durations in Fig. 6.2a, b are less than 32 μs, and increase with increasing N. Thus the contact force *impulse* varies with N.

⇝ *The physical phenomenon that is responsible for this observed and simulated behavior, is the presence of nonlinear waves inside the column of beads during the shock. These waves create some energy dispersion inside the chain.*

It is noteworthy that due to the property of sphere/sphere collisions, waves inside the bodies (bulk waves) are negligible (the impacts are quasi-static, see Sect. 4.2.4). Thus an excellent model of the chain, consists of particles interacting with Hertz stiffness (and some damping, the choice of which is crucial and not straightforward). What happens during and after the shock? In a monodisperse chain (all identical, lossless spheres) that is impacted by one of these spheres at one end (this is the "classical" Newton's cradle case study), the waves due to the local deformations of the beads take the form of an almost-perfect solitary wave that travels through the chain (until it arrives at the last "free" bead, which thus takes almost all of the initial kinetic energy). In case of a chain colliding a ground, the wave effects are much less regular.

6.1.1.1 Discontinuity w.r.t. Initial Conditions

The fact that the impact outcome (the postimpact velocities) may depend on the way the system is initialized, has been noticed a long time ago [422]. This is directly related with the order of the pairwise collisions at the various contact points, and to the kinetic angles between the hypersurfaces of constraints. Consider for instance a chain as in Fig. 6.1, with $N = 2$, masses m_1 and m_2, radii R_1 and R_2, coordinates q_1 and q_2, respectively. Its dynamics is given by:

$$\begin{cases} m_1\ddot{q}_1(t) = -m_1 g + \lambda_{12}(t) \\ m_2\ddot{q}_2(t) = -m_2 g - \lambda_{12}(t) + \lambda_2(t) \\ \\ 0 \le \lambda_{12} \perp f_1(q) = q_1 - q_2 - R_1 - R_2 \ge 0 \\ 0 \le \lambda_2 \perp f_2(q) = q_2 - R_2 \ge 0, \end{cases} \tag{6.1}$$

where λ_{12} is the force exerted by ball 1 on ball 2, λ_2 is the force exerted by the wall on ball 2. The impact dynamics is given by:

$$\begin{cases} m_1(\dot{q}_1(t_k^+) - \dot{q}_1(t_k^-)) = p_1(t_k) \\ m_2(\dot{q}_2(t_k^+) - \dot{q}_2(t_k^-)) = -p_1(t_k) + p_2(t_k). \end{cases} \tag{6.2}$$

We associate a Newton's impact law with each contact, with restitution coefficients $e_{\mathrm{n},1}$ and $e_{\mathrm{n},2}$, respectively. The superscript $-$ means pre-impact velocity, whereas $+$ means postimpact velocity. When there are several impacts we indicate it as $++$ or $+++$. The sequence of impacts B_2/wall (Σ_2) and B_1/B_2 (Σ_1) produces the outcome

$$\begin{cases} \dot{q}_1^+ = \frac{m-e_{\mathrm{n},1}}{1+m}\dot{q}_1^- - e_{\mathrm{n},2}\frac{1+e_{\mathrm{n},1}}{1+m}\dot{q}_2^- \\ \\ \dot{q}_2^{++} = \frac{m(1+e_{\mathrm{n},1})}{1+m}\dot{q}_1^- - e_{\mathrm{n},2}\frac{1-e_{\mathrm{n},1}m}{1+m}\dot{q}_2^-, \end{cases} \tag{6.3}$$

with $m \stackrel{\Delta}{=} \frac{m_1}{m_2}$. The sequence of impacts B_1/B_2 (Σ_1) and B_2/wall (Σ_2) and then B_1/B_2 (Σ_1) again, produces the outcome[1]:

$$\begin{cases} \dot{q}_1^{++} = \frac{m-e_{\mathrm{n},1}}{1+m}\left(\frac{m-e_{\mathrm{n},1}}{1+m}\dot{q}_1^- + \frac{1+e_{\mathrm{n},1}}{1+m}\dot{q}_2^-\right) - e_{\mathrm{n},2}\frac{1+e_{\mathrm{n},1}}{1+m}\left(\frac{m(1+e_{\mathrm{n},1})}{1+m}\dot{q}_1^- + \frac{1-e_{\mathrm{n},1}m}{1+m}\dot{q}_2^-\right) \\ \\ \dot{q}_2^{+++} = \frac{m(1+e_{\mathrm{n},1})}{1+m}\left(\frac{m-e_{\mathrm{n},1}}{1+m}\dot{q}_1^- + \frac{1+e_{\mathrm{n},1}}{1+m}\dot{q}_2^-\right) - e_{\mathrm{n},2}\frac{1-e_{\mathrm{n},1}m}{1+m}\left(\frac{m(1+e_{\mathrm{n},1})}{1+m}\dot{q}_1^- + \frac{1-e_{\mathrm{n},1}m}{1+m}\dot{q}_2^-\right). \end{cases} \tag{6.4}$$

Clearly, the final values in (6.3) and (6.4) are not the same. Let us provide a second example on a 3-ball chain as in Fig. 6.4, but where the initial gap between ball 1 and ball 2 is δ_1 and the initial gap between ball 2 and ball 3 is δ_2. Suppose that $\dot{q}_1(t_k^-) = v_s > 0$, $\dot{q}_3(t_k^-) = -v_s < 0$, and $\dot{q}_2(t_k^-) = 0$. Also let us choose $m_1 = m_3 = \frac{m}{4}$ and $m_2 = m$. If $\delta_1 < \delta_2$, one computes the outcome $\dot{q}_1(t_k^+) = -\frac{6v_s}{10}$ m/s, $\dot{q}_2(t_k^+) = -\frac{4v_s}{25}$ m/s, $\dot{q}_3(t_k^+) = \frac{31v_s}{25}$ m/s. Now if $\delta_1 > \delta_2$, one computes the outcome $\dot{q}_1(t_k^+) = -\frac{31v_s}{25}$ m/s, $\dot{q}_2(t_k^+) = \frac{4v_s}{25}$ m/s, $\dot{q}_3(t_k^+) = \frac{3v_s}{5}$ m/s. The problem is perfectly symmetric, and one expects that if $\delta_1 = \delta_2$ the outcome is also symmetric. Energy conservation yields $\dot{q}_1(t_k^+) = -v_s$ m/s, $\dot{q}_3(t_k^+) = v_s$ m/s, $\dot{q}_2(t_k^+) = 0$ m/s. One sees that if the impact occurs as a double impact (i.e. right at the codimension 2 singularity of the admissible domain boundary), it is impossible to deduce it from the limit of the impacts that occur in an arbitarily small neighborhood of this singularity. This

[1] It is implicitly assumed here that there exists initial velocities and positions such that these various sequences of collisions exist, incorporating the kinematic admissibility of the postimpact velocities.

second example shows that continuity in the initial data (see Sect. 1.3.2.3) may not hold for systems with multiple unilateral constraints.

$\rightsquigarrow$ *Multiple surfaces of constraints (equivalently codimension* ≥ 2 *boundaries of the admissible domain* Φ*) may create discontinuity of the solutions with respect to the initial conditions. In this case, it is not possible to deduce the impact law at the singularity (simultaneous impacts) by studying the limit as the initial data approach the singularity.*

This explains why binary collision models have to be used with some care.

6.1.1.2 Momentum Conservation

It is often taken for granted that the conservation of momentum (linear momentum for a chain of aligned balls) is part of an impact law. Such a point of view is absolutely wrong. Indeed, the conservation of linear momentum at an impact time, is a direct consequence of Newton's third law of action/reaction: *When one body exerts a force on a second body, the second body simultaneously exerts a force equal in magnitude and opposite in direction on the first body*. One has to assume that Newton's third law is still valid during collisions, which seems to be a reasonable assumption, though historically subject to some controversy [434]. To illustrate this fact, consider the dynamics of the 3-ball system as in Fig. 6.4, where the balls have radii R. Its dynamics outside impacts is given by:

$$\left\{\begin{array}{l} m_1\ddot{q}_1(t) = -\lambda_{12}(t) \\ m_2\ddot{q}_2(t) = \lambda_{12}(t) - \lambda_{23}(t) \\ m_3\ddot{q}_3(t) = \lambda_{23}(t) \\ \\ f_1(q) = q_2 - q_1 - 2R \geq 0 \\ f_2(q) = q_3 - q_2 - 2R \geq 0. \end{array}\right. \tag{6.5}$$

Let us notice that both (6.1) and (6.5) fit within (5.1). Clearly from (6.5) one has $m_1\ddot{q}_1(t) + m_2\ddot{q}_2(t) + m_3\ddot{q}_3(t) = 0$, from which it follows that the linear momentum satisfies $m_1\dot{q}_1(t)+m_2\dot{q}_2(t)+m_3\dot{q}_3(t) = m_1\dot{q}_1(0)+m_2\dot{q}_2(0)+m_3\dot{q}_3(0)$. This property is kept at the impact time, as shown in (6.9) that yields $m_1\dot{q}_1(t_k^+) + m_2\dot{q}_2(t_k^+) + m_3\dot{q}_3(t_k^+) = m_1\dot{q}_1(t_k^-) + m_2\dot{q}_2(t_k^-) + m_3\dot{q}_3(t_k^-)$. Such is not the case for (6.1), whose impact dynamics is in (6.2).

$\rightsquigarrow$ *The linear momentum may or may not be conserved at an impact. The fact that conservation holds for the 3-ball system, is just an* illustration *of momentum conservation on a specific system. It is not part of any impact law.*

The last point is illustrated in the next section. Historically, Newton's third law has been used for the first time to solve an impact problem, by 'sGravesand in 1721 [1091], who also suspected that plastic deformation could play a role. Leibniz was the first to use kinetic energy conservation together with what we call today Newton's restitution law (with $e_n = 1$) [434].

6.1.1.3 Single Versus Multiple Impacts

Let us make some computations which clarify the major discrepancy between single and multiple impacts. Let us consider the 3-ball system, with initial conditions $\dot{q}_1(t_k^-) = 1$ m/s, $\dot{q}_2(t_k^-) = \dot{q}_3(t_k^-) = 0$ m/s, ball 2 and ball 3 touch each other initially, $m_1 = m_2 = m_3 = 1$ g. The set of equalities and inequalities which have to hold at the impact time t_k are

$$\begin{cases} \dot{q}_1(t_k^+) - 1 = -p_{12}(t_k) \\ \dot{q}_2(t_k^+) = p_{12}(t_k) - p_{23}(t_k) \\ \dot{q}_3(t_k^+) = p_{23}(t_k) \\ \\ p_{23}(t_k) \geq 0,\ p_{12}(t_k) \geq 0 \quad \text{(kinetic constraints)} \\ \\ \nabla f_1(q)^T \dot{q}(t_k^+) = \dot{q}_2(t_k^+) - \dot{q}_1(t_k^+) \geq 0 \\ \nabla f_2(q)^T \dot{q}(t_k^+) = \dot{q}_3(t_k^+) - \dot{q}_2(t_k^+) \geq 0 \quad \text{(kinematic constraints)} \\ \\ \dot{q}_1(t_k^+)^2 + \dot{q}_2(t_k^+)^2 + \dot{q}_3(t_k^+)^2 = 1 \quad \text{(energetic constraint).} \end{cases} \tag{6.6}$$

It follows from the post-velocities admissibility that $\dot{q}_3(t_k^+) \geq \dot{q}_2(t_k^+) \geq \dot{q}_1(t_k^+)$. From the energy constraint $|\dot{q}_1(t_k^+)^2| \leq 1$ so that $p_{12}(t_k) = 1 - \dot{q}_1(t_k^+) \geq 0$. Assume that $\dot{q}_3(t_k^+) \leq 0$, then $\dot{q}_2(t_k^+) \leq 0$ and $\dot{q}_1(t_k^+) \leq 0$: this is impossible from the linear momentum conservation equation $\dot{q}_1(t_k^+) + \dot{q}_2(t_k^+) + \dot{q}_3(t_k^+) = 1$. Thus necessarily $\dot{q}_3(t_k^+) > 0$, hence $p_{23}(t_k) > 0$: the kinetic constraints are automatically satisfied if the other equalities and inequalities hold. We may therefore eliminate the impulses *via* the momentum conservation and solve the problem with velocities only. We are left with the system:

$$\begin{cases} \dot{q}_1(t_k^+) + \dot{q}_2(t_k^+) + \dot{q}_3(t_k^+) = 1 \\ \dot{q}_1(t_k^+)^2 + \dot{q}_2(t_k^+)^2 + \dot{q}_3(t_k^+)^2 = 1 \\ \dot{q}_2(t_k^+) - \dot{q}_1(t_k^+) \geq 0, \quad \dot{q}_3(t_k^+) - \dot{q}_2(t_k^+) \geq 0. \end{cases} \tag{6.7}$$

It happens that the system in (6.7) possesses an infinity of solutions, which are "between" two "extremals": (A) with $(\dot{q}_1(t_k^+), \dot{q}_2(t_k^+), \dot{q}_3(t_k^+)) = (0, 0, 1)$ and (B) with $(\dot{q}_1(t_k^+), \dot{q}_2(t_k^+), \dot{q}_3(t_k^+)) = (-\frac{1}{3}, \frac{2}{3}, \frac{2}{3})$ (see Fig. 6.3b).
Let us consider now the impact between two balls. Doing a similar reasoning it is easy to obtain the system:

$$\begin{cases} \dot{q}_1(t_k^+) + \dot{q}_2(t_k^+) = 1 \\ \dot{q}_1(t_k^+)^2 + \dot{q}_2(t_k^+)^2 = 1 \\ \dot{q}_2(t_k^+) - \dot{q}_1(t_k^+) \geq 0. \end{cases} \tag{6.8}$$

The system in (6.8) has a unique solution $\dot{q}_1(t_k^+) = 0$ m/s, $\dot{q}_2(t_k^+) = 1$ m/s. Imposing Newton's impact law with $e_n = 1$ implies the energy equality, see (4.41). On the other hand, imposing $T_L(t_k) = 0$ and the kinematic constraint implies $e_n = 1$.

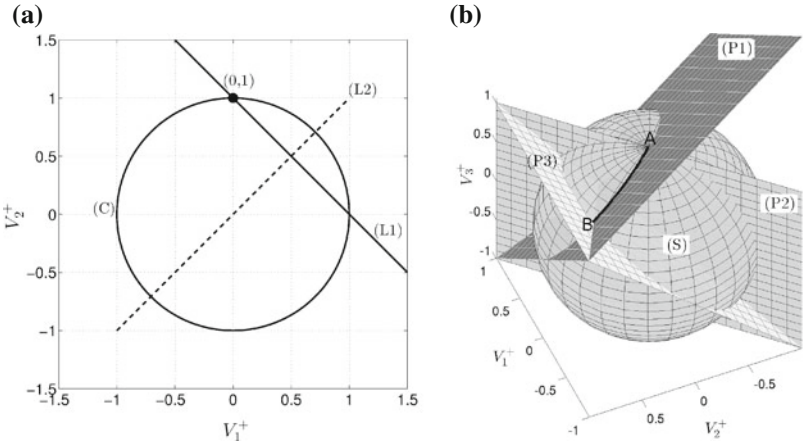

Fig. 6.3 Post-impact velocities domains ($V_i^+ \stackrel{\Delta}{=} \dot{q}_i(t_k^+)$). Taken from [929, Figs. 1.1 and 1.2]. **a** System in (6.8). **b** System in (6.7)

Graphically, the two systems in (6.7) and (6.8) are depicted in Fig. 6.3. In Fig. 6.3b, momentum conservation defines the plane (P_1) is defined from the points $(0, 0, 1)$, $(0, 1, 0)$ and $(1, 0, 0)$. Energy constraint defines the boundary of the sphere. The kinematic constraints impose that the postimpact velocities must be located in front of (P_2) and above (P_3)

$\rightsquigarrow$ *Energy conservation (or a simple impact law) is sufficient to make the impact problem solvable with uniqueness for the central impact of two balls. It is not sufficient to solve with uniqueness the 3-ball system at impact: a multiple impact law is needed. The set of solutions of* (6.7) *corresponds to various dispersions of the kinetic energy in the chain after the collision.*

6.1.1.4 Kinetic Energy Dispersion

The outcome of the central impact between two spheres of masses m_1 and m_2, where friction is neglected (an assumption that we obviously made from the beginning of this section), where $\dot{q}_1(t_k^-) = 1$ m/s and $\dot{q}_2(t_k^-) = 0$ m/s, and energy is conserved, is given using (4.42) by $\dot{q}_1(t_k^+) = \dot{q}_1(t_k^-) - 2\frac{m_2(\dot{q}_1(t_k^-)-\dot{q}_2(t_k^-))}{m_1+m_2} = 1 - \frac{2m_2}{m_1+m_2}$, and $\dot{q}_2(t_k^+) = \dot{q}_2(t_k^-) + 2\frac{m_1(\dot{q}_1(t_k^-)-\dot{q}_2(t_k^-))}{m_1+m_2} = \frac{2m_1}{m_1+m_2}$. Consider now a chain of M aligned identical balls in contact, that impacts a second chain of N identical balls which are also in contact (we may call this an $M : N$-collision). Suppose that $m_1 = Mm$, $m_2 = Nm$, where m is the mass of each ball. If the balls of each sub-chain are glued together (and hence are equivalent to two solid rigid bodies), one obtains the outcome $\dot{q}_1(t_k^+) = \frac{M-N}{M+N}$ and $\dot{q}_2(t_k^+) = \frac{2M}{M+N}$. It is noteworthy that this result holds if a Hertz or linear stiffness is used to model the contact/impact between the two

spheres. Indeed these compliant models yield an equivalent restitution coefficient $e_n = 1$, while energy and momentum (more exaclty, Newton's third law) constraints are unchanged. Thus the kinetic energy of the balls that move forward after the collision, is equal to $\frac{1}{2}Nm\left(\frac{2M}{M+N}\right)^2$ if $N \geq M$ (only ball 2 moves forward), and to $\frac{1}{2}Nm\left(\frac{2M}{M+N}\right)^2 + \frac{1}{2}Mm\left(\frac{M-N}{M+N}\right)^2$ if $N < M$ (both balls move forward). What happens when the balls are not glued, but the contacts are unilateral? Extensive simulations with Hertz unilateral springs[2] are presented in [749, Table II] for $M + N = 10$ balls. They show that as the number of impacting balls M increases, there are $M + 2$ balls that move forward after the shock (with positive velocity), while the remaining balls on the left move backwards with very low negative velocities. Moreover the postimpact kinetic energy of the $M + 2$ "forward" balls is approximately 99 % of the total kinetic energy. Both systems (glued contacts and unilateral contacts) match if and only if $M + 2 = N$ and $N\left(\frac{2M}{N+M}\right)^2 = 0.99M$. This holds if and only if $M = 9$ and $N = 11$. The results are therefore in general quite different one from each other. The reason is that the deformations at the contacts, and the unilaterality, allow the creation of wave phenomena through the chain of $N+M$ balls during the impact. The nonlinear waves are quite irregular ones except if $M = 1$, even if the two sub-chains are monodisperse. They are responsible for the dispersion (or the distribution) of the energy within the chain after the collision. Similar numerical results on $M : N$ collisions with $M + N = 50$ and 100, $N = 1, 2, 3, 4, 5, 6$ are presented in [529, § 5 (c)]. They show that there are M separated solitary waves which are created through the chain, and which are responsible for the balls to fly off after the impact, each solitary wave acting as a "collisional effect" for the last ball. The longer the chain, the more separated the waves. They also show that when $N = 5$ and $M = 1, 2, 3, 4$, then $M + 1$ balls move forward after the collision while the remaining ones move backwards with very small velocities.

$\rightsquigarrow$ *Once again, nonlinear waves make the impacts in chains of balls—and more generally in multibody systems—a quite complex phenomenon. The design of a rigid-body-like model of multiple impacts, that would encapsulate such wave effects, is a hard task.*

Remark 6.2 The dispersion effect, is sometimes named the *distance effect*. Indeed if the collision is assumed to be instantaneous, the impact at one edge of the chain produces an effect at the other edge.

To be complete, we should also consider impacts between two elastic bodies, like sphere/rod or rod/rod collisions, and compare the results with the above. The type of elasticity, and the type of waves (planar displacement linear wave traveling along the rods) is quite different from the nonlinear waves in chains of balls with unilateral Hertz elasticity. Roughly speaking, linear waves in elastic rods follow the 1 dimensional linear wave equation $\frac{\partial^2 u}{\partial t^2} = c^2 \frac{\partial^2 u}{\partial x^2}$, where $u(t, x)$ is the displacement of the rod's thin section, $c = \sqrt{\frac{E}{\rho}}$ is the speed of the uniform planar displacement wave,

[2] Which do represent an excellent, high-fidelity model for impacting spheres [387].

E is the rod's Young modulus and ρ its density. They may be considered as the limit of chains with bilateral, linear springs, when the number of elements tends to infinity (a spatial discretization of the linear wave equation). While nonlinear waves in chains of aligned balls follow nonlinear partial differential equations [609], and there may exist solitary waves in $1 : N$ collisions of monodisperse chains [1087]. These solitons have doubly exponential decay [275], so that they are concentrated on a compact support of five balls in long enough chains.

$\rightsquigarrow$ *The linear waves—bulk vibrational effects—in elastic bodies, and the nonlinear waves in chains of balls with unilateral Hertzian contact, are of quite different nature.*

6.1.1.5 Equivalence of Rheological Compliant Models

When two bodies collide, two contact compliant models (visco-elastic, or elasto-plastic) which provide the same restitution coefficient will give the same postimpact velocity. From this point of view, they are equivalent, despite they may provide quite different impact duration and contact force history. If the same compliant models are used in a chain of balls to model the contact between each pair of balls, the postimpact velocity of the balls may however drastically differ. The reason is that despite they give the same restitution coefficient for pairwise collisions, the contact force history, the impact duration and the maximum compression times that they predict, may differ. These discrepancies may in turn produce quite different impact outcomes, see Sect. 6.1.3 for the lossless case.

6.1.2 Han-Gilmore's and Binary Collisions Models

Let us start with the method proposed by Han and Gilmore [500] that is an analytical computer-oriented method to analyze multiple impacts, including friction. The method in [500] does not apply to closed kinematic-loops, but is rather devoted to granular-like systems. The authors analyze the outcomes in multibody systems when some contacts may break, due to *internal impacts* (see definition below). A computational algorithm is presented, based on a particular topological description of the system: the distance k between contact-impact points is chosen to be the minimum number of bodies that separate a given point and the prespecified reference point. The algorithm uses the impact analysis between two bodies developed in [500] to calculate, for each k (starting at $k = 0$) the postimpact motion. Then an exhaustive procedure that considers all possible outcomes during the impact process is given. Let us note that it is not stated in [500] that the proposed algorithm yields a solution in all cases, and if it does whether it is unique or not. As the simple 3-ball system shows in Sect. 6.1.3, uniqueness cannot be expected in general (the example we treat corresponds to the perfectly elastic case; when the perfectly plastic case is chosen—$e_{\mathrm{n}} = 0$ at both contacts—then Han and Gilmore algorithm converges in an infinite number of iterations [372], see also Sect. 6.1.4 below). A 5-ball system of elastic beads—$e_{\mathrm{n}} = 1$ at all contacts—is analysed in [929, p. 57] with non unique outcome.

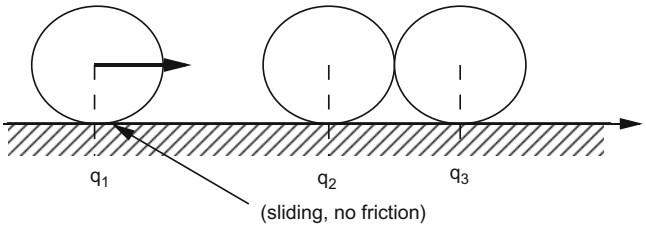

Fig. 6.4 The 3-ball system

Let us consider the system depicted in Fig. 6.4. The three balls (or spheres, or particles) are sliding horizontally. There is no dissipation between the balls and the ground. The notion of *internal* and *sequential* impacts is introduced in [500]: internal impacts are impacts that occur between two bodies previously in contact, i.e. which occur in fact through an internal transmission inside the bodies, and such that they create detachment.[3] The authors also assume the possibility of a certain chronology for the possible impacts occuring in the system, hence sequential impacts. Although such an analysis might appear natural for the treatment of multiple collisions, it will be shown that multiple impact phenomena require deeper analysis because sequential pairwise impacts are not sufficient to model them properly. Let us explain how solutions (i.e. postimpact velocities) can be found. The shock dynamical equations are given at the shock instant t_k by:

$$\left\{\begin{array}{l} \dot{q}_1(t_k^+) - \dot{q}_1(t_k^-) = -p_{12}(t_k) \\ \dot{q}_2(t_k^+) - \dot{q}_2(t_k^-) = p_{12}(t_k) - p_{23}(t_k) \\ \dot{q}_3(t_k^+) - \dot{q}_3(t_k^-) = p_{23}(t_k). \end{array}\right. \tag{6.9}$$

The masses are taken equal to one for simplicity, and the pre-impact velocities are chosen as $\dot{q}_1(t_k^-) = 1, \dot{q}_2(t_k^-) = \dot{q}_3(t_k^-) = 0$. It is supposed no energy loss ($T_L(t_k) = 0$) at impacts. Two postimpact sets of velocities are computed and are given by:

$$\dot{q}_1(t_k^+) = -\tfrac{1}{3},\ \dot{q}_2(t_k^+) = \dot{q}_3(t_k^+) = \tfrac{2}{3}\ \text{m/s}, \tag{6.10}$$

and

$$\dot{q}_1(t_k^+) = \dot{q}_3(t_k^+) = 0,\ \dot{q}_2(t_k^+) = 1\ \text{m/s}. \tag{6.11}$$

The solution in (6.10) can be found by applying Newton's restitution rule with $e_n = 1$ between bodies 1 and 2 (i.e. $\dot{q}_1(t_k^+) = -1 + \dot{q}_2(t_k^+)$), and between bodies 2 and 3 (i.e. $\dot{q}_2(t_k^+) = \dot{q}_3(t_k^+)$), and assuming a nonzero $p_{23}(t_k)$ (i.e. implicitly assuming a nonzero $\dot{q}_3(t_k^+)$). The solution in (6.11) can be found by assuming no shock between bodies 2 and 3, i.e. $p_{23}(t_k) = 0$. Now notice that (6.10) can be set as definitive since postimpact motion is possible: the first body rebounds and the other two remain stuck.

[3] Internal impacts are due to distance effects, created by waves that travel through the multibody system.

But solution 2 is not feasible between bodies 2 and 3: that problem is overcome in [500] by assuming a second impact between bodies 2 and 3. Applying Newton's rule between bodies 1 and 2 and bodies 2 and 3 yields another nonfeasible solution. But assuming there is no impact between 1 and 2 (i.e. $p_{12}(t_k) = 0$) yields a feasible motion. This solution is then given by:

$$\dot{q}_1(t_k^{++}) = \dot{q}_2(t_k^{++}) = 0,\ \dot{q}_3(t_k^{++}) = 1 \text{ m/s}. \tag{6.12}$$

The superscript $^{++}$ is to distinguish the impacts chronologically. This solution is a possible motion: bodies 1 and 2 remain stuck, body 3 moves to the right. In fact the above reasoning relies on three rules:

- (i) The kinetic energy loss at impact is zero (energy constraint).
- (ii) The postimpact velocity must assure a feasible motion, i.e. point inwards the domain inside the constraints (kinematic constraint).
- (iii) Let us denote q_i and q_{i+1} the coordinates of two successive balls. Then if $\dot{q}_i(t_k^-) > \dot{q}_{i+1}(t_k^-)$, the percussion between these two bodies $p_{ij} \neq 0$. If $\dot{q}_i(t_k^-) < \dot{q}_{i+1}(t_k^-)$, $p_{ij} = 0$. If $\dot{q}_i(t_k^-) = \dot{q}_{i+1}(t_k^-)$, then two possibilities must be tested: either $p_{ij}(t_k) = 0$ or $p_{ij}(t_k) > 0$ (kinetic constraint).

It can be shown that due to the particular choice of the initial conditions, (i) implies that the restitution coefficients between the balls is equal to 1. (ii) allows one to decide at each step whether a computed velocity is admissible or not. (iii) is a fundamental rule which permits to decide the form of the percussion vector. It can be shown that in this particular example, the algorithm has a finite number of iterations, and that the only two possible postimpact velocities are the ones in (6.10) and (6.12). When an admissible velocity has been found, it is considered as definitive. But all possible paths have to be tested.

Thus the Han and Gilmore algorithm yields two possible solutions for the postimpact velocities, and it is *a priori* impossible to decide which one is the right one, just relying on rigid body theory. Experimentally, monodisperse 3-ball chains with balls made of very hard material, evolve closely to the solution in (6.12). However the experimental outcome is different: although the third ball detaches quickly from the second one and takes about 98 % of the kinetic energy, the second and the first balls possess nonzero postimpact velocity, and do have a motion after the shock (for instance, values $\dot{q}_1(t_k^+) = -0.0605\dot{q}_1(t_k^-)$ m/s, $\dot{q}_2(t_k^+) = 0.1049\dot{q}_1(t_k^-)$ m/s and $\dot{q}_3(t_k^+) = 0.9978\dot{q}_1(t_k^-)$ m/s are reported from experiments in [985]). This is related to kinetic energy dispersion inside the chain. The balls are commonly made of hard material (iron) so that the rigid body assumption can be considered to be valid in this case. However the small postimpact motion of the first and second balls should not be neglected because it has a great influence on the long-term dynamics of the chain.

Close to the Han and Gilmore algorithm is the so-called *binary collision model*. One starts assuming that the impacts are pairwise and sequential with an *a priori* given order (e.g. for the 3-ball chain, a first impact between ball 1 and ball 2, then a second impact between ball 2 and ball 3). The first collision gives a first postimpact velocity $\dot{q}(t^+)$. One has to check whether $\nabla f(q)^T \dot{q}(t^+) \geq 0$, which implies that the

three balls do not collide again. If this condition is not satisfied, then another impact occurs that gives $\dot{q}(t^{++})$. One then checks if $\nabla f(q)^T \dot{q}(t^{++}) \geq 0$ or not, and so on. Such binary collision approach may yield an accumulation of impacts in a finite time. Moreover it is meant to correctly model the wave effect inside the chain, but does not always provide satisfactory results. Finally, changing the initial sequence of impacts may change the final outcome, because of discontinuity of the trajectories with respect to initial data, as shown in (6.2)–(6.4). For the 3-ball chain, one obtains the following results. Let us assume that $\dot{q}_1(t_0^-) = \dot{q}_1^0 > 0$ m/s, $\dot{q}_2(t_0^-) = \dot{q}_3(t_0^-) = 0$ m/s, and that there is a first impact between balls 1 and 2, then between balls 2 and 3. One obtains [929]:

$$\begin{cases} \dot{q}_1(t_0^{++}) = \dfrac{1-\dfrac{m_2}{m_1}e_{\mathrm{n},1}}{1+\dfrac{m_2}{m_1}}\dot{q}_1^0 \\ \dot{q}_2(T_0^{++}) = \dfrac{(1-\dfrac{m_3}{m_2}e_{\mathrm{n},2})(1+\dfrac{m_2}{m_1}e_{\mathrm{n},1})}{(1+\dfrac{m_2}{m_1})(1+\dfrac{m_3}{m_2})}\dot{q}_1^0 \\ \dot{q}_3(t_0^{++}) = \dfrac{(1+e_{\mathrm{n},1})(1+e_{\mathrm{n},2})}{(1+\dfrac{m_2}{m_1})(1+\dfrac{m_3}{m_2})}\dot{q}_1^0. \end{cases} \tag{6.13}$$

For a monodisperse conservative chain ($e_{\mathrm{n},1} = e_{\mathrm{n},2} = 1$, $m_1 = m_2 = m_3$), the outcome $\dot{q}_1(t_0^{++}) = \dot{q}_2(t_0^{++}) = 0$ and $\dot{q}_3(t_0^{++}) = \dot{q}_1^0$ m/s is found, that corresponds to (6.12). If $e_{\mathrm{n},1} = e_{\mathrm{n},2} = 0$ then $\dot{q}_1(t_0^{++}) = \frac{\dot{q}_1^0}{2}$ m/s, $\dot{q}_2(t_0^{++}) = \dot{q}_3(t_0^{++}) = \frac{\dot{q}_1^0}{4}$ m/s: it does not satisfy the criterion $\nabla f(q)^T \dot{q}(t^{++}) \geq 0$, thus other impacts have to be calculated. It happens that the postimpact velocities outcome domain when both $e_{\mathrm{n},1}$ and $e_{\mathrm{n},2}$ are varied between 0 and 1, does not fill in the whole quarter disk in Fig. 5.5, but just the portion of it denoted (II), see [929, Fig. 3.7]. It is therefore not clear why in general it should be preferred to Moreau's rule, which is much simpler to implement in a code. Experiments on the 2-ball system hitting a wall (take $N = 2$ in Fig. 6.1), are performed in [126] with varying initial gap between the two balls (this is known as the basketball-tennis ball problem[4]). It is shown that as the initial gap becomes very small (the collision approaches a 2-impact), then prediction of binary collision model and experimental results diverge significantly [126, Fig. 3]. It is also striking that the impact duration for positive gap, is quite different from the impact duration for nearly zero gap [126, Fig. 9]. It is shown also in [982] that the binary collision model is valid for certain range of mass and stiffness ratios only: *this proves, if needed, that multiple impacts involve internal mechanisms related to wave effects, which may significantly depart from sequential, binary collisions*. Fundamentally, the fact that the balls' gap is strictly positive, or if it vanishes, drastically modifies

[4] An experiment anyone can do. Put a tennis ball on the top of a basketball, and drop both on a rigid ground. The tennis ball rebounds violently and very high, while the basketball almost does not rebound at all: the whole energy is transferred to the tennis ball during the impact with the ground.

the impact wave that travels through the balls. Further results on the basketball-tennis ball problem, may be found in [315, 906]. It is noteworthy that both balls are shells with internal pressure, and may not obey Hertz' elasticity, nor classical damping (see [751, Sect. 8] and [126]).

Remark 6.3 The analysis of multiple impacts using binary collision models, is closely related to the study of impacts of a particle in a two-dimensional wedge, and to the analysis of billiards. Indeed the 3-ball system is equivalent, after some suitable transformation, to a particle striking a corner, see [929, Appendix A] for a complete analysis. See also Sect. 6.1.4.

6.1.3 Penalization at Contacts (Compliance)

Let us consider the 3-ball system as depicted in Fig. 6.5. The study which follows may be seen as an extension of the contents of Sect. 2.1.1, in a multiple impact context. The dynamical equations are given by:

$$\begin{cases} m_1\ddot{x}_1(t) = k_1(x_2(t) - x_1(t)) \\ m_2\ddot{x}_2(t) = k_1(x_1(t) - x_2(t)) + k_2(x_3(t) - x_2(t)) \\ m_3\ddot{x}_3(t) = k_2(x_2(t) - x_3(t)) \\ x_1(0) = x_2(0) = x_3(0) = 0,\ \dot{x}_1(0) = 1\ m/s, \dot{x}_2(0) = \dot{x}_3(0) = 0\ m/s. \end{cases} \tag{6.14}$$

Let us denote $k_1 = k$, $\frac{k_2}{k_1} = \gamma$, $m_1 = m_2 = m_3 = m$, $\Delta = \sqrt{\gamma^2 - \gamma + 1}$, $\alpha_1 = \sqrt{-\Delta + \gamma + 1}$, $\alpha_2 = \sqrt{\Delta + \gamma + 1}$, $\omega = \sqrt{\frac{k}{m}}$, $\omega_1 = \alpha_1\omega$, $\omega_2 = \alpha_2\omega$. The solution of (6.14) is given by:

$$\begin{cases} x_1(t) = \frac{1}{\omega_1}\left(\frac{1}{3} - \frac{1-2\gamma}{6\Delta}\right)\sin(\omega_1 t) + \frac{1}{\omega_2}\left(\frac{1}{3} + \frac{1-2\gamma}{6\Delta}\right)\sin(\omega_2 t) + \frac{t}{3} \\ x_2(t) = -\frac{1}{\omega_1}\left(\frac{1}{6} - \frac{2-\gamma}{6\Delta}\right)\sin(\omega_1 t) - \frac{1}{\omega_2}\left(\frac{1}{6} + \frac{2-\gamma}{6\Delta}\right)\sin(\omega_2 t) + \frac{t}{3} \\ x_3(t) = -\frac{1}{\omega_1}\left(\frac{1}{6} + \frac{1+\gamma}{6\Delta}\right)\sin(\omega_1 t) - \frac{1}{\omega_2}\left(\frac{1}{6} - \frac{1+\gamma}{6\Delta}\right)\sin(\omega_2 t) + \frac{t}{3}. \end{cases} \tag{6.15}$$

The balls 1 and 2 separate at time t_1 such that $x_1(t_1) = x_2(t_1)$, and the balls 2 and 3 separate at time t_2 such that $x_3(t_2) = x_2(t_2)$, with:

$$\begin{cases} (\Delta - 1 - \gamma)\alpha_2 \sin(\omega_1 t_1) + (\Delta + 1 - \gamma)\alpha_1 \sin(\omega_2 t_1) = 0 \\ \alpha_2 \sin(\omega_1 t_2) - \alpha_1 \sin(\omega_2 t_2) = 0. \end{cases} \tag{6.16}$$

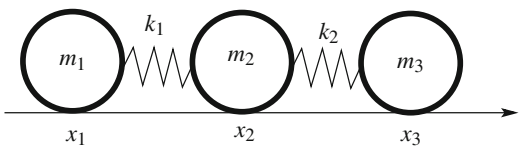

Fig. 6.5 Three-ball system with unilateral elastic contacts

It is noteworthy that the solutions $\omega_1 t_1, \omega_2 t_1, \omega_1 t_2$ and $\omega_2 t_2$ of these two transcendental equations, do not depend on k since their coefficients do not depend on k.

$\rightsquigarrow$ *Thus from* (6.15) *it follows that the velocities at separation times, are independent of* k, *but depend only on the stiffness ratio* γ.

This was already noticed in [202, 203], as well as in [622, 623] for the two-ball system hitting a wall (for which the outcome depends also on the mass ratio only). Let us now study two extreme cases, where $\gamma = 0$ and $\gamma = +\infty$. In the first case $\gamma = 0$, one can show that $\omega_1 = 0$, $\omega_2 = \sqrt{2}\omega$, $\sin(\omega_2 t_1) = 0$ and $t_1 = \frac{\pi}{\sqrt{2}\omega}$ (compare with (2.2)). Consequently, $t_1 < t_2$ and $\dot{x}_1(t_1) = 0$ m/s, $\dot{x}_2(t_1) = 1$ m/s, $\dot{x}_3(t_1) = 0$ m/s. Therefore, balls 2 and 3 continue their collision, and it is easily obtained that at the end of this collision (which is the end of the multiple shock) one has $\dot{x}_1(t_f) = 0$ m/s, $\dot{x}_2(t_f) = 0$ m/s, $\dot{x}_3(t_f) = 1$ m/s. When $\gamma = +\infty$ we find $\omega_1 = \omega$, $\omega_2 = +\infty$, $\sin(\omega_1 t_1) = 0$, $\sin(\omega_1 t_2) = 0$, $t_1 = t_2 = \frac{\pi}{\omega}$ (compare again with (2.2): this time the 2-impact behaves like a single impact!). Then $\dot{x}_1(t_f) = -\frac{1}{3}$ m/s, $\dot{x}_2(t_f) = \dot{x}_3(t_f) = \frac{2}{3}$ m/s. This last outcome is the one obtained applying Moreau's impact law (or Newton's impact law at each contact) with a CoR $e_n = 1$, see Example 5.5. It is important to see that these two extreme cases, can be obtained by letting the stiffnesses k_1 and k_2 both diverge to infinity, but at different rates. This proves that even in the limit of a rigid body model, the outcome of this multiple impact depends strongly on the relative stiffnesses, though they do not depend on the absolute value of the stiffnesses. It is noteworthy that the two extreme cases for the stiffness ratio γ, give the solutions in (6.10) and (6.12).

$\rightsquigarrow$ *The energetical behavior of the system, plus the kinetic and kinematic constraints, are not sufficient to characterize the impact outcome in a multiple impact. The results of the lossless, penalized 3-ball system when the stiffness ratio* γ *varies, confirms the analysis of Sect.* 6.1.1.3: *varying* γ *allows to span the portion of arc* AB *in Fig.* 6.3*b; in Fig.* 5.5, *it allows to span the curve* AB *for* $KER = 1$, *while Moreau's law is "stuck" at* B.

More calculations with different assumptions on the parameters, may be found in [929, Appendix C].

Remark 6.4 (*Zero Dispersion Chains*) We consider the initial velocities in (6.14). Reinsch [1035] has shown that a symmetric chain of $n + 1$ aligned beads, with unilateral linear elastic contacts, is totally *dispersion-free* (that is, the last bead takes exactly all the energy of the impacting one, and the other beads have zero postimpact velocity) if the masses and the stiffnesses are properly chosen [929, Appendix D]. For a 3-ball chain, one finds equal stiffnesses $k_1 = k_2$ and $m_1 = m_3 = m$, $m_2 = \frac{2}{3}m$. Newby [632] investigates a 3-ball chain with equal masses, and whether it is possible to recover γ from the postimpact velocities (this is called in [632] the *inverse scattering* problem): this is not always possible. He finds that all possible postimpact outcomes are described with compliant models such that $\gamma \in (0, \gamma_{\max})$, for some $\gamma_{\max}$. There is therefore a periodicity in γ in the dynamics. In particular the solution $\dot{x}_1(t_f) = -\frac{1}{3}$ m/s, $\dot{x}_2(t_f) = \dot{x}_3(t_f) = \frac{2}{3}$ m/s, occurs for an infinite number of γ's,

not only for $\gamma = \infty$. Newby also finds that balls 1 and 2 separate at the same time as balls 2 and 3 (a sort of symmetrical double collision with $t_1 = t_2$) when $\gamma = \frac{(3n^4-2n^2+3)+\sqrt{9n^8-12n^6-42n^4-12n^2+9}}{8n^2}$, $n = 2, 3, 4 \ldots$.

6.1.4 Multiplicity of Multiple Impacts

When a particle hits an angle in the plane, it may rebound successively on both the surfaces in various ways, depending on the CoRs and the angle value. This is a binary collision model including possible secondary impacts, which gives outcomes for collision that occur near the singularity (a 2-impact in the sense of Definition 6.1). Let us summarize here the results of Towne and Hadlock [1211], who deal with a three-ball chain (that is equivalent to the particle hitting an angle, see [929, Sect. A.1]). The two Newton's CoRs are chosen equal ($e_{\mathrm{n},1} = e_{\mathrm{n},2} = e_{\mathrm{n}}$). The first ball collides the two other balls at rest. The number of collisions and the postimpact velocities depend on the following variable:

$$z = \zeta(e_{\mathrm{n}})\eta(m_{1,2}, m_{3,2}), \tag{6.17}$$

where $\zeta(e_{\mathrm{n}})$ and $\eta(m_{1,2}, m_{3,2})$ are defined as:

$$\begin{cases} \zeta(e_{\mathrm{n}}) = \frac{1}{2}\left(\sqrt{e_{\mathrm{n}}} + \frac{1}{\sqrt{e_{\mathrm{n}}}}\right) \geq 1 & \text{for all } e_{\mathrm{n}} \in (0, 1] \\ \eta(m_{1,2}, m_{3,2}) = \frac{1}{\sqrt{(1+m_{2,1})(1+m_{2,3})}} < 1 & \text{for all } m_{1,2},\ m_{3,2}, \end{cases} \tag{6.18}$$

with $m_{j,i} = m_j/m_i$. We see that $z > 0$ and can diverge to infinity as $e_{\mathrm{n}} \to 0$. The variable z consists of two distinct parts $\zeta(e_{\mathrm{n}})$ and $\eta(m_{1,2}, m_{3,2})$: $\zeta(e_{\mathrm{n}})$ is related to the dissipative behavior of the chain, while $\eta(m_{1,2}, m_{3,2})$ is related to the kinetic angle θ_{12} of the chain defined by $\eta(m_{1,2}, m_{3,2}) = \cos(\theta_{12})$ (this can be calculated from (6.66), see [929, Eq. (A.4)]). The number of binary collisions is given as follows:

- When $0 < z < 1$, the number of collisions N is finite and computed as:

$$N = \left\lfloor \frac{\pi}{\arccos(z)} - 1 \right\rfloor \tag{6.19}$$

- When $z \geq 1$, the number of collisions N is infinite.

The above results show that $N \leq 3$ when $z > 1/2$, i.e. secondary collisions occur when $z > 1/2$. Moreover, the number of collisions N increases as z increases and it becomes infinite when $z \geq 1$. Consider the case when $e_{\mathrm{n}} = 1 \ \Rightarrow \ z = \cos(\theta_{12})$. From (6.19), the number N of collisions is given by:

$$N = \left\lfloor \frac{\pi - \theta_{12}}{\theta_{12}} \right\rfloor. \tag{6.20}$$

The condition for which N is infinite ($z \geq 1$) can be rewritten as:

$$\frac{1}{2}\left(\sqrt{e_{\mathrm{n}}} + \frac{1}{\sqrt{e_{\mathrm{n}}}}\right)\cos(\theta_{12}) \geq 1. \tag{6.21}$$

More on this topic may be found in [683, 936], see also [929, § 3.4, Appendix A]. Extending this type of analysis to $e_{\mathrm{n},1} \neq e_{\mathrm{n},2}$ or to more than three balls (equivalently, to particles in three dimensions hitting a "pyramidal" angle), seems to be at best very difficult.[5] It nevertheless shows that the binary collision model may indeed involve, even in simple systems, an infinity of successive impacts. If this infinity occurs in a finite time, a Zeno phenomenon occurs which may create difficulty for time-integration with an event-driven code.

6.2 Kinematic Multiple-Impact Law (Generalized Newton)

This section is devoted to investigate how we may extend kinematic impact laws like Newton's or Moreau's laws, in order to obtain an impact law which is able to span the whole set of admissible outcomes. To this aim we proceed with a particular transformation of the Lagrange equations in (5.1).

6.2.1 The Quasi-Lagrange Equations

Let us remind that the m_b bilateral constraints are denoted as $h_i(q)$ for $i \in \{1, \ldots, m_b\}$, and the m_u unilateral constraints are $f_i(q) \geq 0$ for $i \in \{m_{b+1}, \ldots, m_u + m_b\}$, and we assume that $m_u + m_b \leq n$. We also assume that $M(q) \succ 0$, and all the constraints $f_i(q)$ and $h_i(q)$ are functionally independent at any $q \in \mathscr{Q}$, that is the $(m_u + m_b) \times n$ gradient matrix $\begin{pmatrix} \nabla f(q) \\ \nabla h(q) \end{pmatrix}$ has full column rank $m_u + m_b$. This in particular precludes that the gradients vanish in the domain of interest on the configuration space $\mathscr{Q}$. The $m_u + m_b$ normal unitary vectors to the codimension 1 constraints manifolds $\Sigma_i = \{q \in \mathscr{Q} | h_i(q) = 0\}$, $1 \leq i \leq m_b$, equipped with the kinetic metric are defined as:

$$\mathbf{n}_{q,i} = \frac{M^{-1}(q)\nabla h_i(q)}{\sqrt{\nabla h_i^T(q) M^{-1}(q) \nabla h_i(q)}}, \quad 1 \leq i \leq m_b, \tag{6.22}$$

and similarly for $\Sigma_i = \{q \in \mathscr{Q} | f_i(q) = 0\}$, $m_b + 1 \leq i \leq m_b + m_u$. Clearly the normal vectors $\mathbf{n}_{q,i} \in \mathbb{R}^n$ are independent. If $m_b + m_u < n$ we have to complete the

[5] It has to the best of the author's knowledge, never been tackled, despite Towne and Hadlock's article was published in 1977.

set $(\mathbf{n}_{q,1}, \ldots, \mathbf{n}_{q,m+p})$ by $n - m_b - m_u$ mutually independent vectors $\mathbf{t}_{q,i}$ in order to make a basis. The $\mathbf{t}_{q,i}$ vectors are chosen such that $\langle \mathbf{t}_{q,i}, \mathbf{n}_{q,j} \rangle_q = \mathbf{t}_{q,i}^T M(q) \mathbf{n}_{q,j} = 0$ for all $i \in \{1, \ldots, n - m_u - m_b\}$, $j \in \{1, \ldots, m_u + m_b\}$. We notice that the vectors $\mathbf{t}_{q,i}^T$ are orthogonal to the kinetic gradients $\mathbf{n}_{q,j}$ in the kinetic metric, and orthogonal to the Euclidean gradients $\nabla h_i(q)$ and $\nabla f_i(q)$ in the Euclidean metric. One may choose unitary vectors $\mathbf{t}_{q,i}$, i.e. $\mathbf{t}_{q,i}^T M(q) \mathbf{t}_{q,i} = 1$. Therefore the vectors $\mathbf{t}_{q,i}$ span $T_q \mathcal{Q}$ whereas the vectors $\mathbf{n}_{q,i}$ span the normal cone $N_\Phi(q)$ to the admissible domain Φ of $\mathcal{Q}$. This admissible domain for q is defined as follows: $\Phi \stackrel{\Delta}{=} \Phi_b \times \Phi_u$ with $\Phi_b = \{q \in \mathcal{Q} | h_i(q) = 0, i \in \{1, \ldots, m_b\}\}$ and $\Phi_u = \{q \in \mathcal{Q} | f_i(q) \geq 0, i \in \{m_b + 1, \ldots, m_b + m_u\}\}$. Thus Φ_b is the bilateral holonomic constraints manifold with codimension m, $\Phi_b = \cap_{i=1}^{m_b} \Sigma_i$, whereas Φ_u is the admissible domain defined by the unilateral constraints, $\Phi_u = \cap_{i=m_b+1}^{m_b+m_u} \Phi_{u,i}$, with $\Phi_{u,i} = \{q \in \mathcal{Q} | f_i(q) \geq 0, i \in \{m_b + 1, \ldots, m_b + m_u\}\}$. For obvious reasons we assume that Φ_u contains a ball of radius > 0. One has $N_\Phi(q) = N_{\Phi_b}(q) \times N_{\Phi_u}(q)$, where $N_{\Phi_b}(q) = \{w \in \mathbb{R}^n | w = \sum_{i=1}^{m_b} \alpha_i \mathbf{n}_{q,i}, \alpha_i \in \mathbb{R}\}$ is the normal cone in the kinetic metric.

6.2.1.1 Frictionless Systems

Let us define the $n \times n$ matrix $\Xi(q) = \begin{pmatrix} \mathbf{n}_q^T \\ \mathbf{t}_q^T \end{pmatrix}$, where $\mathbf{n}_q = (\mathbf{n}_{q,1}, \ldots, \mathbf{n}_{q,m_u+m_b})$ and $\mathbf{t}_q = (\mathbf{t}_{q,1}, \ldots, \mathbf{t}_{q,n-m_u-m_b})$. The *kinetic quasi-velocities* are defined as:

$$v \stackrel{\Delta}{=} \begin{pmatrix} \dot{q}_{\text{norm}} \\ \dot{q}_{\text{tan}} \end{pmatrix} = \Xi(q) M(q) \dot{q} \tag{6.23}$$

where the notation norm and tan come from the fact that v in (6.23) is the Euclidean projection of the generalized momentum $p = M(q)\dot{q}$ on the basis $\mathbf{n}_q$ and $\mathbf{t}_q$ (equivalently the projection of $\dot{q}$ on $\mathbf{n}_q$ and $\mathbf{t}_q$ in the kinetic metric). One could therefore call the kinetic quasi-velocities, the *mass-projected momentum*. From (6.23) $\dot{q}_{\text{norm}} = \mathbf{n}_q^T M(q) \dot{q}$ has dimension $m_u + m_b$ and $\dot{q}_{\text{tan}} = \mathbf{t}_q^T M(q) \dot{q}$ has dimension $n - m_u - m_b$. Notice that the $(m_u + m_b) \times n$ matrix $\mathbf{n}_q^T M(q)$ has rows $\frac{\nabla h_i^T(q)}{||\nabla h_i(q)||_{M^{-1}}}$ and $\frac{\nabla f_i^T(q)}{||\nabla f_i(q)||_{M^{-1}}}$. Thus it follows that $\dot{q}_{\text{norm},i} = \frac{\nabla h_i^T(q) \dot{q}}{||\nabla h_i(q)||_{M^{-1}}}$, and $\mathbf{n}_q = M^{-1}(q)(\nabla h(q), \nabla f(q)) \text{diag}\left(\frac{1}{||\nabla h_i(q)||_{M^{-1}}}, \frac{1}{||\nabla f_i(q)||_{M^{-1}}}\right)$.

Remark 6.5 The developments presented in this section extend the material in the first and second editions of this book [202, 203], and have been investigated in [210, 228]. The use of the kinetic metric for the study of multiple impacts was perhaps first advocated in [581]. It is also implicitly present in Moreau's works [890, 894] where the tangent and normal cones are defined in a generic way, independently of the metric, see also [454, § 4]. The kinetic metrix is also used in mathematical

proofs for convergence of numerical schemes [375]. Notice that far as one analyses the system at a fixed q (like for impacts), then $M(q)$ is constant and the metric is Euclidean.

Example 6.1 For the rocking block system in Sect. 6.3.2.2, we have: $\dot{q}_{\text{norm},1} = \frac{\dot{y}+(\frac{l}{2}\sin(\theta)+\frac{L}{2}\cos(\theta))\dot{\theta}}{\sqrt{\frac{1}{m}+\frac{1}{4I_G}(l\sin(\theta)+L\cos(\theta))^2}}$, $\dot{q}_{\text{norm},2} = \frac{\dot{y}+(\frac{l}{2}\sin(\theta)-\frac{L}{2}\cos(\theta))\dot{\theta}}{\sqrt{\frac{1}{m}+\frac{1}{4I_G}(l\sin(\theta)+L\cos(\theta))^2}}$, $\dot{q}_{\text{tan}} = \sqrt{m}\dot{x}$. For a monodisperse chain of four aligned balls with mass m and radius R, $f_1(q) = q_2 - q_1 - 2R \geq 0$, $f_2(q) = q_3 - q_2 - 2R \geq 0$, $f_3(q) = q_4 - q_3 - 2R \geq 0$. Therefore $\nabla f_1(q) = (-1\ 1\ 0\ 0)^T$, $\nabla f_2(q) = (0\ -1\ 1\ 0)^T$, $\nabla f_3(q) = (0\ 0\ -1\ 1)^T$. After some calculations one finds $\dot{q}_{\text{norm},1} = \frac{1}{\sqrt{2m}}(-\dot{q}_1 + \dot{q}_2)$, $\dot{q}_{\text{norm},2} = \frac{1}{\sqrt{2m}}(-\dot{q}_2 + \dot{q}_3)$, $\dot{q}_{\text{norm},3} = \frac{1}{\sqrt{2m}}(-\dot{q}_3 + \dot{q}_4)$, and $\dot{q}_{\text{tan}} = \frac{\sqrt{m}}{2}(\dot{q}_1 + \dot{q}_2 + \dot{q}_3 + \dot{q}_4)$. It becomes clear from these two examples that in general, $\dot{q}_{\text{tan}}$ does not correspond to the "real-world" tangent velocity at contact points: generalized and local point of views may not match.

Let us denote $F(q, \dot{q}, t) \stackrel{\Delta}{=} C(q, \dot{q})\dot{q} + G(q) - F_{ext}$ in (5.1). Let us now perform the kinetic quasi-velocity transformation of the constrained Lagrange dynamics (5.1) with $H_{\text{t},u}(q, t)\lambda_{\text{t},u} + H_{\text{t},b}(q, t)\lambda_{\text{t},b} = 0$. First notice that:

$$\begin{pmatrix} \ddot{q}_{\text{norm}} \\ \ddot{q}_{\text{tan}} \end{pmatrix} = \Xi(q)M(q)\ddot{q} + \frac{d}{dt}(\Xi(q)M(q))\dot{q} \tag{6.24}$$

Pre-multipyling both sides of (5.1) (a) by $\Xi(q)$ and grouping the normal multipliers as $\lambda_{\text{n}} = \begin{pmatrix} \lambda_{\text{n},b} \\ \lambda_{\text{n},u} \end{pmatrix}$, one obtains:

$$\begin{pmatrix} \ddot{q}_{\text{norm}} \\ \ddot{q}_{\text{tan}} \end{pmatrix} + \Xi(q)F(q, \dot{q}, t) - \frac{d}{dt}(\Xi(q)M(q))\dot{q} = \begin{pmatrix} \mathbf{n}_q^T(\nabla h(q), \nabla f(q))\lambda_{\text{n}} \\ \mathbf{t}_q^T(\nabla h(q), \nabla f(q))\lambda_{\text{n}} \end{pmatrix} \tag{6.25}$$

Let us define $\bar{\lambda}_{\text{n}}$ such that $\bar{\lambda}_{\text{n},b,i} \stackrel{\Delta}{=} ||\nabla h_i(q)||_{M^{-1}}\lambda_{\text{n},b,i}$, $\bar{\lambda}_{\text{n},u,i} \stackrel{\Delta}{=} ||\nabla f_i(q)||_{M^{-1}}\lambda_{\text{n},u,i}$, i.e. $\bar{\lambda}_{\text{n}} = \text{diag}(||\nabla h_i(q)||_{M^{-1}}, ||\nabla f_i(q)||_{M^{-1}})\lambda_{\text{n}}$.[6] From the definition of $\mathbf{t}_{q,i}$ it follows that $\mathbf{t}_q^T(\nabla h(q), \nabla f(q))\lambda_{\text{n}} = 0$, therefore (6.25) becomes:

$$\begin{aligned} &\ddot{q}_{\text{norm}}(t) + F_{\text{norm}}(q(t), \dot{q}_{\text{norm}}(t), \dot{q}_{\text{tan}}(t), t) = [\mathbf{n}_q(t)^T M(q(t))\mathbf{n}_q(t)]\ \bar{\lambda}_{\text{n}}(t) \\ &\ddot{q}_{\text{tan}}(t) + F_{\text{tan}}(q(t), \dot{q}_{\text{norm}}(t), \dot{q}_{\text{tan}}(t), t) = 0 \end{aligned} \tag{6.26}$$

[6] Notice that the assumption that the constraints are functionally independent, guarantees that the norms $||\nabla h_i(q)||_{M^{-1}}$ and $||\nabla f_i(q)||_{M^{-1}}$ never vanish, so $\text{diag}(||\nabla h_i(q)||_{M^{-1}}, ||\nabla f_i(q)||_{M^{-1}})$ is positive definite.

with obvious definitions for $F_{\text{norm}}(q, \dot{q}_{\text{norm}}, \dot{q}_{\text{tan}}, t)$ and $F_{\text{tan}}(q, \dot{q}_{\text{norm}}, \dot{q}_{\text{tan}}, t)$. This canonical form of the dynamics is remarkable because it splits the velocities in a "normal" and a "tangential" parts, similarly to the case of a particle hitting a single frictionless constraint: this is a *generalized particle dynamics*. This is however at the price of introducing additional nonlinearities (stemming from the constraints) in the inertial generalized forces (see the left-hand side in (6.25)). The terms indexed by tan are not affected by the contact force and may be thought of as some kind of tangential dynamics. We may choose to call the first line of (6.26) the *quasi-normal dynamics* and the second line the *quasi-tangential dynamics*. The dynamics in (6.23) (6.26) is consequently a particular case of:

$$\begin{cases} \dot{q}(t) = A(q(t))^{-1} v(t) \\ \bar{M}(q(t))\dot{v}(t) = G(q(t), v(t), t) + A(q(t))^{-T} H(q(t))\lambda \\ v = A(q)\dot{q}, \end{cases} \tag{6.27}$$

where $G(q, v, t)$ gathers inertial forces (centrifugal, Coriolis), forces that derive from the potential energy (gravity, elasticity), external and dissipative forces (control inputs, disturbances, Raileygh dissipation), the mass matrix $\bar{M}(q)$ in (6.27) is not necessarily equal to $M(q)$, v has dimension n, $A(q)$ is invertible but not necessarily integrable, and $H(q)\lambda$ groups all contact forces in the right-hand side of (5.1). In other words, there does not necessarily exist any *quasi-position* $\bar{q} = g(q)$ such that $\frac{d\bar{q}}{dt} = \frac{\partial g}{\partial q}(q)\dot{q}$, so that $A(q)$ is not the Jacobian of any mapping $g(q)$. It is clear that v may correspond to some non-holonomic constraints, hence the name non-holonomic velocities that is sometimes given to quasi-velocities.

It is clear that (6.26) usually is not a Lagrange dynamics since $\bar{M}$ is constant (the identity) whereas nonlinear inertial forces do not vanish (such dynamics are sometimes called Lagrange's equations in quasi-velocities, or Boltzmann-Hamel equations [155], and they may be written in a Lagrangian-like form [367, 417]). Remind that the Delassus' matrix defined when $m_b = 0$ (only unilateral constraints) is equal to $\nabla f(q)^T M(q)^{-1} \nabla f(q)$. The matrix $\mathbf{n}_q^T M(q) \mathbf{n}_q$ may be seen as a normalized Delassus' matrix,[7] whose diagonal entries are equal to 1. It is positive definite if and only if $\mathbf{n}_q$ has full rank $m_u + m_b$. Notice that we can split $\dot{q}_{\text{norm}}$ as $\dot{q}_{\text{norm}} = \begin{pmatrix} \dot{q}^b_{\text{norm}} \\ \dot{q}^u_{\text{norm}} \end{pmatrix}$ with $\dot{q}^b_{\text{norm}} \in \mathbb{R}^{m_b}$ corresponds to bilateral constraints, and $\dot{q}^u_{\text{norm}} \in \mathbb{R}^{m_u}$ corresponds to unilateral constraints. Similarly one has

$$\mathbf{n}_q^T M(q) \mathbf{n}_q = \begin{pmatrix} \mathbf{n}_q^{b,T} M(q) \mathbf{n}_q^b & \mathbf{n}_q^{b,T} M(q) \mathbf{n}_q^u \\ \mathbf{n}_q^{u,T} M(q) \mathbf{n}_q^b & \mathbf{n}_q^{u,T} M(q) \mathbf{n}_q^u \end{pmatrix} \tag{6.28}$$

[7] The Delassus' operator is sometimes called the *fundamental matrix* [185].

Thus the first line in (6.26) can be rewritten as (we drop the time argument in the right-hand side):

$$\begin{cases} \ddot{q}^b_{\text{norm}}(t) + F^b_{\text{norm}}(q(t), \dot{q}_{\text{norm}}(t), \dot{q}_{\text{tan}}(t), t) = \mathbf{n}_q^{b,T} M(q) \mathbf{n}_q^b \bar{\lambda}_{\text{n},b} + \mathbf{n}_q^{b,T} M(q) \mathbf{n}_q^u \bar{\lambda}_{\text{n},u} \\ \ddot{q}^u_{\text{norm}}(t) + F^u_{\text{norm}}(q(t), \dot{q}_{\text{norm}}(t), \dot{q}_{\text{tan}}(t), t) = \mathbf{n}_q^{u,T} M(q) \mathbf{n}_q^b \bar{\lambda}_{\text{n},b} + \mathbf{n}_q^{u,T} M(q) \mathbf{n}_q^u \bar{\lambda}_{\text{n},u} \end{cases} \tag{6.29}$$

Since $\dot{q}^b_{\text{norm}} = 0$ at all times because the system evolves on the codimension $2m_b$ manifold $\{q \in \mathscr{Q} | h_i(q) = 0, \nabla h_i^T(q)\dot{q} = 0, i \in \{1, \ldots, m_b\}\}$, the first equation in (6.29) is equal to $F^b_{\text{norm}}(q, \dot{q}^u_{\text{norm}}, \dot{q}_{\text{tan}}, t) = \mathbf{n}_q^{b,T} M(q) \mathbf{n}_q^b \bar{\lambda}_{\text{n},b} + \mathbf{n}_q^{b,T} M(q) \mathbf{n}_q^u \bar{\lambda}_{\text{n},u}$. If the $m_b \times m_b$ matrix $\mathbf{n}_q^{b,T} M(q) \mathbf{n}_q^b$ is invertible one may obtain λ_n^b from this equation and insert it into the second equation in (6.29) to obtain a dynamics that no longer depends on $\bar{\lambda}_{\text{n},b}$. This modifies the unilateral part of the dynamics (and in particular one obtains a new Delassus' matrix given in (6.35) below). A detailed analysis of the couplings between unilateral and bilateral constraints is made in [209].

6.2.1.2 Systems with Friction

We now incorporate the generalized forces $H_{\text{t}}(q)\lambda_{\text{t}} \stackrel{\Delta}{=} H_{\text{t},u}(q,t)\lambda_{\text{t},u} + H_{\text{t},b}(q,t)$ $\lambda_{\text{t},b} = 0$ in the analysis. Then (6.26) becomes:

$$\begin{aligned} &\ddot{q}_{\text{norm}} - \tfrac{d}{dt}(\mathbf{n}_q^T M(q))\dot{q} + \mathbf{n}_q^T F(q, \dot{q}, t) = \mathbf{n}_q^T M(q) \mathbf{n}_q \ \bar{\lambda}_n + \mathbf{n}_q^T H_{\text{t}}(q) \ \lambda_{\text{t}} \\ &\ddot{q}_{\text{tan}} - \tfrac{d}{dt}(\mathbf{t}_q^T M(q))\dot{q} + \mathbf{t}_q^T F(q, \dot{q}, t) = \mathbf{t}_q^T H_{\text{t}}(q) \ \lambda_{\text{t}} \end{aligned} \tag{6.30}$$

It is remarkable in (6.30) that there is no reason in general that $\mathbf{n}_q^T H_{\text{t}}(q) = 0$, i.e. $\mathbf{n}_q$ is not in general an anihilator of $H_{\text{t}}(q)$. This means that the quasi-tangential dynamics may influence the quasi-normal dynamics, but the reverse never holds since by construction of the basis $(\mathbf{n}_q, \mathbf{t}_q)$ one has $\mathbf{t}_q^T \nabla h(q) = \mathbf{t}_q^T \nabla f(q) = 0$. This is what makes the strong difference between systems with normal/tangential couplings (like the Painlevé example analysed in Sect. 5.6), and systems without normal/tangential couplings. We may say that *generalized particles dynamics usually have normal/tangential inertial couplings, with* $\mathbf{n}_q^T H_{\text{t}}(q) \neq 0$.

6.2.2 The Kinetic Energy

Clearly $\dot{q}^b_{\text{norm}}$ does not play any role in the kinetic energy, being zero. We will see later that the same applies to $\dot{q}_{\text{tan}}$ when one considers the kinetic energy variation at

an impact. Let us assume that $\Xi(q)$ has full rank n. One has:

$$\Xi(q)M(q)\Xi^T(q) = \begin{pmatrix} \mathbf{n}_q^T \\ \mathbf{t}_q^T \end{pmatrix} M(q)(\mathbf{n}_q \ \mathbf{t}_q) = \begin{pmatrix} \mathbf{n}_q^T M(q)\mathbf{n}_q & 0 \\ 0 & \mathbf{t}_q^T M(q)\mathbf{t}_q \end{pmatrix}, \quad (6.31)$$

from which one deduces the inverse matrix:

$$\Xi^{-T}(q)M^{-1}(q)\Xi^{-1}(q) = \begin{pmatrix} (\mathbf{n}_q^T M(q)\mathbf{n}_q)^{-1} & 0 \\ 0 & (\mathbf{t}_q^T M(q)\mathbf{t}_q)^{-1} \end{pmatrix} \quad (6.32)$$

which holds provided the normalized Delassus' matrix has full rank n. Now we have:

$$\begin{aligned} T(q,\dot{q}) &= \tfrac{1}{2}\dot{q}^T M(q)\dot{q} = \tfrac{1}{2}\dot{q}^T M(q)\Xi^T(q)\Xi^{-T}(q)M^{-1}(q)\Xi^{-1}(q)\Xi(q)M(q)\dot{q} \\ &= \tfrac{1}{2}v^T \begin{pmatrix} (\mathbf{n}_q^T M(q)\mathbf{n}_q)^{-1} & 0 \\ 0 & (\mathbf{t}_q^T M(q)\mathbf{t}_q)^{-1} \end{pmatrix} v \\ &= \tfrac{1}{2}\dot{q}_{\text{norm}}^T(\mathbf{n}_q^T M(q)\mathbf{n}_q)^{-1}\dot{q}_{\text{norm}} + \tfrac{1}{2}\dot{q}_{\tan}^T(\mathbf{t}_q^T M(q)\mathbf{t}_q)^{-1}\dot{q}_{\tan} = T(q,v) \end{aligned} \quad (6.33)$$

Now one may use (6.28) and the Schur complement [218, § A.5] to deduce:

$$T(q,\dot{q}) = \tfrac{1}{2}\dot{q}_{\text{norm}}^{u,T} G^{-1}(q)\dot{q}_{\text{norm}}^{u} + \tfrac{1}{2}\dot{q}_{\tan}^T(\mathbf{t}_q^T M(q)\mathbf{t}_q)^{-1}\dot{q}_{\tan} \quad (6.34)$$

with:

$$G(q) = \mathbf{n}_q^{u,T} M(q)\mathbf{n}_q^u - \mathbf{n}_q^{u,T} M(q)\mathbf{n}_q^b(\mathbf{n}_q^{b,T} M(q)\mathbf{n}_q^b)^{-1}\mathbf{n}_q^{b,T} M(q)\mathbf{n}_q^u \quad (6.35)$$

We see that this matrix has the same structure as $\tilde{D}_{bu}(q(t),t)$ in (5.20), and represents the distorsion of the Delassus' matrix due to bilateral constraints. Due to the assumption that the constraints are independent, $G(q)$ has full rank and is even positive definite.[8] If $m_b = 0$ (no bilateral constraints) and $m_u = 1$, then $\dot{q}_{\text{norm}}^u = \dot{q}_{\text{norm}}$ and one recovers the result in [203, Eq. (6.11)] that $T(q,\dot{q}) = \frac{1}{2}\dot{q}_{\text{norm}}^2 + \frac{1}{2}\dot{q}_{\tan}^T(\mathbf{t}_q^T M(q)\mathbf{t}_q)^{-1}\dot{q}_{\tan}$.

It is noteworthy that the basis $(\mathbf{n}_q, \mathbf{t}_q)$ is not orthonormal, because the vectors $\mathbf{n}_{q,i}$, $i \in \{1,\ldots,m_b+m_u\}$, and $\mathbf{t}_{q,i}$, $i \in \{1,\ldots,n-m_b-m_u\}$ are not necessarily orthogonal to one another (except if the constraints are orthogonal). Thus,

[8] Its properties are studied in [209, § 4] without noticing, anyway, that it is a Schur complement.

despite the quasi-mass matrix $\bar{M}(q)$ in (6.26) is the identity, the kinetic energy in (6.34) does not have the simple form $2T(q, v) = v^T v$ as is for instance the case in [155, Eq. (20)].

6.2.3 The Contact Forces Power

6.2.3.1 Normal Contact Forces Power

Let $F_{\mathrm{n}}(q) \stackrel{\Delta}{=} \nabla f(q)\lambda_{\mathrm{n}}$. Let us investigate now the power performed by the generalized contact force: $\mathscr{P}_{\mathrm{n}} = F_{\mathrm{n}}^T(q)\dot{q}$ where $\dot{q}$ is assumed to be compatible with the bilateral and the unilateral constraints (i.e. we consider virtual velocities $\dot{q}$ such that the virtual displacement $\delta q = \dot{q}dt$ is compatible with the constraints and such that the virtual work is $\mathscr{W}_{\mathrm{n}} = \mathscr{P}_{\mathrm{n}}dt$). Then from the above developments we obtain:

$$\begin{aligned}\mathscr{P}_{\mathrm{n}} &= F_{\mathrm{n}}(q)^T\dot{q} = \lambda_{\mathrm{n}}^T\nabla f(q)^T\dot{q} = \lambda_{\mathrm{n}}^T \mathrm{diag}(||\nabla h_i(q)||_{M^{-1}}, ||\nabla f_i(q)||_{M^{-1}})\mathbf{n}_q^T M(q)\dot{q}\\ &= \bar{\lambda}_{\mathrm{n}}^T\mathbf{n}_q^T M(q)\dot{q} = \bar{\lambda}_{\mathrm{n}}^T\dot{q}_{\mathrm{norm}} = \bar{\lambda}_{\mathrm{n},u}^T\dot{q}_{\mathrm{norm}}^u,\end{aligned} \tag{6.36}$$

where we used that $\dot{q}_{\mathrm{norm}}^b = 0$ always. Now, one has $0 \leq \lambda_{\mathrm{n},u} \perp f(q) \geq 0$, therefore if the system lies in the interior of the admissible domain Φ_u one has $\lambda_{\mathrm{n},u} = 0$ and $\mathscr{P}_{\mathrm{n}} = 0$. If the system evolves smoothly on a part of the boundary $\mathrm{bd}(\Phi_u)$ that is finitely represented by the active constraints indexed in $\mathscr{J}(q)$, one has $0 \leq \dot{q}_{\mathrm{norm,i}} \perp \lambda_{\mathrm{n},u,i} \geq 0$ for all $i \in \mathscr{J}(q)$. Consequently in this case also $\mathscr{P}_{\mathrm{n}} = 0$. Since the constraints are all perfect, the power developed by the contact forces outside possible impacts is always zero, as expected. The interest of (6.36) is to highlight the fact that the "forces" that perform work on the quasi-velocities $\dot{q}_{\mathrm{norm}}^u$ are the multipliers $\bar{\lambda}_{\mathrm{n},u}$.

Let us denote $F_{\mathrm{norm}}^{\mathrm{n}}(q) \stackrel{\Delta}{=} \mathbf{n}_q^T M(q)\mathbf{n}_q\bar{\lambda}_{\mathrm{n}}$ and $D_{\mathrm{n}}(q) \stackrel{\Delta}{=} (\mathbf{n}_q^T M(q)\mathbf{n}_q)^{-1}$. Then from (6.36) one gets:

$$\mathscr{P}_{\mathrm{n}} = \bar{\lambda}_{\mathrm{n}}^T\dot{q}_{\mathrm{norm}} = \langle F_{\mathrm{norm}}^{\mathrm{n}}(q), \dot{q}_{\mathrm{norm}}\rangle_{D_{\mathrm{n}}} \tag{6.37}$$

Let us also denote $D_{\mathrm{t}}(q) \stackrel{\Delta}{=} (\mathbf{t}_q^T M(q)\mathbf{t}_q)^{-1}$.[9] As a result, one finds that the frictionless Lagrangian system with a set of holonomic bilateral and unilateral constraints is equivalently represented as a generalized particle with dynamics:

$$\begin{cases}\ddot{q}_{\mathrm{norm}}(t) + F_{\mathrm{norm}}(q, \dot{q}_{\mathrm{norm}}(t), \dot{q}_{\mathrm{tan}}(t), t) = F_{\mathrm{norm}}^{\mathrm{n}}(q(t))\\ \ddot{q}_{\mathrm{tan}}(t) + F_{\mathrm{tan}}(q, \dot{q}_{\mathrm{norm}}(t), \dot{q}_{\mathrm{tan}}(t), t) = 0\end{cases} \tag{6.38}$$

[9] If the vectors $\mathbf{t}_{q,i}$ are chosen mutually orthogonal then $D_{\mathrm{t}}(q) = I$.

and the kinetic metric $D(q) = \text{diag}(D_{\text{n}}(q), D_{\text{t}}(q))$ (see (6.33)), while $\dot{q}_{\text{norm}} dt$ performs work on $F^{\text{n}}_{\text{norm}}(q)$ in the metric of $D_{\text{n}}(q)$.

6.2.3.2 Tangential Contact Forces Power

Let us compute the virtual power developed by the tangential forces. Let $F_{\text{t}}(q) \stackrel{\Delta}{=} \Xi(q) H_{\text{t}}(q) \lambda_{\text{t}} = \begin{pmatrix} F^{\text{t}}_{\text{norm}}(q) \\ F^{\text{t}}_{\text{tan}}(q) \end{pmatrix}$. Then:

$$\begin{aligned} \mathscr{P}_{\text{t}} &= \dot{q}^T H_{\text{t}}(q) \lambda_{\text{t}} = v^T \Xi^{-T}(q) M^{-1}(q) \Xi^{-1}(q) \Xi(q) H_{\text{t}}(q) \lambda_{\text{t}} \\ &= \langle v, F_{\text{t}}(q) \rangle_D = \langle \dot{q}_{\text{norm}}, F^{\text{t}}_{\text{norm}}(q) \rangle_{D_{\text{n}}} + \langle \dot{q}_{\text{tan}}, F^{\text{t}}_{\text{tan}}(q) \rangle_{D_{\text{t}}} \end{aligned} \tag{6.39}$$

Thus, the total virtual power of the contact forces of the dynamics in (6.30) is equal to:

$$\mathscr{P} = \langle F^{\text{n}}_{\text{norm}}(q), \dot{q}_{\text{norm}} \rangle_{D_{\text{n}}} + \langle \dot{q}_{\text{norm}}, F^{\text{t}}_{\text{norm}}(q) \rangle_{D_{\text{n}}} + \langle \dot{q}_{\text{tan}}, F^{\text{t}}_{\text{tan}}(q) \rangle_{D_{\text{t}}} \tag{6.40}$$

The matrices $D_{\text{n}}(q) \succ 0$ and $D_{\text{t}}(q) \succ 0$ define natural metrics for the system analysed in kinetic quasi-velocities. The coupling between normal and tangential directions appears in the second term in (6.40). There is no orthogonality of the quasi-generalized contact forces $\begin{pmatrix} F^{\text{t}}_{\text{norm}}(q) \\ F^{\text{t}}_{\text{tan}}(q) \end{pmatrix}$ and $\begin{pmatrix} F^{c}_{\text{norm}}(q) \\ 0 \end{pmatrix}$ in the inner product defined by the metric $D(q) \succ 0$. This is in contrast with what happens at the local kinematics level at the contact points. Following Sect. 4.1, let us denote the orthonormal local frame at contact point i as $(\mathbf{n}_i, \mathbf{t}_{i,1}, \mathbf{t}_{i,2})$, with $\mathbf{n}_i \in \mathbb{R}^3, \mathbf{t}_{i,j} \in \mathbb{R}^3$. One has $\langle \mathbf{n}_i, \mathbf{t}_{i,j} \rangle = 0$ in the Euclidean metric. Each contact force can be denoted as $F_i = F_{i,\text{n}} + F_{i,\text{t}}$ with $F_{i,\text{n}} = F_{\text{n},i} \mathbf{n}_i$ and $F_{i,\text{t}} = F_{\text{t},1,i} \mathbf{t}_{i,1} + F_{\text{t},2,i} \mathbf{t}_{i,2}$. The Coulomb's cones are denoted as $\mathscr{C}_i$, with $F_i \in \mathscr{C}_i$. Let $U_i \in \mathbb{R}^3$ be the local velocity, decomposed naturally as $U_i = U_{\text{n},i} + U_{\text{t},i} = u_{\text{n},i} \mathbf{n}_i + u_{\text{t},1,i} \mathbf{t}_{i,1} + u_{\text{t},2,i} \mathbf{t}_{i,2}$. We may thus define virtual local velocities that are compatible with the constraints, and the virtual power at contact i is given by $\mathscr{P}_i = \langle U_i, F_i^c \rangle = \langle U_{i,n}, F_{i,\text{n}} \rangle + \langle U_{i,\text{t}}, F_{i,\text{t}} \rangle$, while

$$\mathscr{P} = \sum_{i=1}^{p} \mathscr{P}_{i,\text{n}} + \mathscr{P}_{i,\text{t}} = \mathscr{P}_{\text{n}} + \mathscr{P}_{\text{t}}. \tag{6.41}$$

Thus, in the local kinematics there is a decoupling between tangential and normal virtual powers, which does not transport very well into generalized frameworks, because of the term $\mathbf{n}_q^T H_{\text{t}}(q)$ in (6.30). Notice that if $u_{\text{n},i} = \nabla f_i(q)^T \dot{q}$, then the multiplier vector λ_{n} satisfies $\lambda_{\text{n},i} = F_{\text{n},i}$, and thus $\mathscr{P}_{\text{n}}$ in (6.36) and $\mathscr{P}_{\text{n}}$ in (6.41) are the same.

6.2.4 Restitution Law for Frictionless Systems

Let us assume for simplicity that there are no bilateral constraints (i.e. $m_b = 0$). Thus $G(q) = D_{\rm n}(q)^{-1}$ and in the sequel we shall use both notations equally. We also assume that $\dot{q}_{\rm norm}$ is constructed from the active constraints at the impact time t_k, i.e. with the constraints whose index belongs to $\mathscr{J}(q(t_k)) = \{i \in \{1,\dots,m_u\} | f_i(q(t_k)) = 0\}$. It is noteworthy that we allow for contacts which are active with zero relative pre-impact velocity (like in a chain of balls or a Newton's cradle). We denote $m'_u = \text{card}(\mathscr{J}(q(t_k)))$. The impact dynamics at an instant t_k such that there is at least one $i \in \{1,\dots,m'_u\}$ such that $\dot{q}_{\text{norm,i}}(t_k^-) < 0$ and $f_i(q(t_k)) = 0$[10] is given by (using (6.26)):

$$\begin{cases} \dot{q}_{\rm norm}(t_k^+) - \dot{q}_{\rm norm}(t_k^-) = \mathbf{n}_q^T M(q)\mathbf{n}_q \ \bar{p}_{\rm n}(t_k) \\ \dot{q}_{\rm tan}(t_k^+) - \dot{q}_{\rm tan}(t_k^-) = 0, \end{cases} \tag{6.42}$$

where $\bar{p}_{{\rm n},i} = ||\nabla f_i(q)||_{M^{-1}} p_{{\rm n},i}$, i.e. $\bar{p}_{\rm n} = \text{diag}(||\nabla f_i(q)||_{M^{-1}}) p_{\rm n}$, and $p_{{\rm n},i}(t_k)$ is the impulse of the contact force multiplier $\lambda_{{\rm n},i}$ at the impact instant t_k. More rigorously $\lambda_{{\rm n},i}$ is a measure at t_k and $p_{{\rm n},i}(t)$ is its density with respect to the Dirac measure at the atom t_k. The role played by the projection of the generalized momentum on the basis $\mathbf{t}_q$ clearly appears in (6.42): the quasi-velocities $\dot{q}_{\rm tan}$ are conserved at the impacts when friction is absent (the constraints are said *perfect*). It is important to notice that despite there may be $\dot{q}_{\text{norm,i}}(t_k^-) = 0$ for some $i \in \mathscr{J}(q(t_k))$, all the terms $\dot{q}_{\text{norm,i}}$, $i \in \{1,\dots,m'_u\}$ may undergo a jump because of the inertial couplings between the constraints, as reflected by the normalized Delassus' matrix $\mathbf{n}_q^T M(q)\mathbf{n}_q$ which is not diagonal in general. It readily follows from the impact dynamics in (6.42) and (6.34) that the kinetic energy loss $T_L(t_k) \stackrel{\Delta}{=} T(q(t_k), \dot{q}(t_k^+)) - T(q(t_k), \dot{q}(t_k^-))$ at a time t_k of impact is given by:

$$T_L(t_k) = \frac{1}{2}\dot{q}^u_{\rm norm}(t_k^+)^T G(q)^{-1}\dot{q}^u_{\rm norm}(t_k^+) - \frac{1}{2}\dot{q}^u_{\rm norm}(t_k^-)^T G(q)^{-1}\dot{q}^u_{\rm norm}(t_k^-) \tag{6.43}$$

where q denotes $q(t_k)$. From now on we will drop the superscript u since there are no bilateral constraints. The framework in (6.42) is suitable to formulate a kinematic impact law as:

$$v(t^+) = \begin{pmatrix} \dot{q}_{\rm norm}(t_k^+) \\ \dot{q}_{\rm tan}(t_k^+) \end{pmatrix} = -\mathscr{E} \begin{pmatrix} \dot{q}_{\rm norm}(t_k^-) \\ \dot{q}_{\rm tan}(t_k^-) \end{pmatrix} \tag{6.44}$$

where $\mathscr{E}$ is a generalized $n \times n$ restitution matrix. Its entries will be named the coefficients of restitution. Let us decompose it as:

$$\mathscr{E} = \begin{pmatrix} \mathscr{E}_{\rm nn} & \mathscr{E}_{\rm nt} \\ \mathscr{E}_{\rm tn} & \mathscr{E}_{\rm tt} \end{pmatrix} \tag{6.45}$$

[10] This is equivalently stated as $\dot{q}(t_k^-) \in -T_{\Phi_u}(q(t_k))$.

with obvious dimensions of the four submatrices: $\mathscr{E}_{\rm nn} \in \mathbb{R}^{m'_u \times m'_u}$, $\mathscr{E}_{\rm tt} \in \mathbb{R}^{(n-m'_u)\times(n-m'_u)}$. In the frictionless case one has $\dot{q}_{\rm tan}(t^+) = \dot{q}_{\rm tan}(t^-)$ for any pre-impact velocity $\dot{q}_{\rm norm}(t^-)$, so necessarily $\mathscr{E}_{\rm tn} = 0$ and $\mathscr{E}_{\rm tt} = -I$. The restitution law in (6.44) is very general as the next result shows:

Proposition 6.1 *Suppose that at least one component of $\dot{q}_{\rm norm}(t_k^-)$ or of $\dot{q}_{\rm tan}(t_k^-)$ is nonzero. Then given any postimpact kinetic quasi-velocity, there exists a value of $\mathscr{E}$ such that (6.44) is satisfied. If at least one component of $\dot{q}_{\rm norm}(t_k^-)$ is negative, then there exists a value of $\mathscr{E}_{\rm nn}$ such that $\dot{q}_{\rm norm}(t_k^+) = -\mathscr{E}_{\rm nn}\dot{q}_{\rm norm}(t_k^-)$.*

Proof Without loss of generality suppose that $v_1(t_k^-) \neq 0$ while $v_i(t_k^-) = 0$ for all $i \geq 2$. Then it suffices to choose $\epsilon_{i1} = -\frac{v_i(t_k^+)}{v_1(t_k^-)}$.

As we know there are three types of consistencies that an impact law has to satisfy: kinematic (admissible postimpact velocities), kinetic (non negative impulses), and energetic.

Proposition 6.2 *Let a frictionless impact occur at t_k. It is necessary and sufficient that:*

- *(i) $\mathscr{E}_{\rm nn}$ is nonnegative (kinematic consistency),*
- *(ii) $G^{-1}(q)(I + \mathscr{E}_{\rm nn})$ is nonnegative (kinetic consistency),*

for $\mathscr{E}_{\rm nn}$ to be an admissible restitution matrix for any pre-impact velocity $\dot{q}_{\rm norm}(t_k^-)$.

Proof (i) assures that $\dot{q}_{\rm norm}(t_k^+) = -\mathscr{E}_{\rm nn}\dot{q}_{\rm norm}(t_k^-) \geq 0$ for any $\dot{q}_{\rm norm}(t_k^-) \leq 0$, (ii) guarantees that $\bar{p}_{\rm n}(t_k) = G(q)^{-1}(\dot{q}_{\rm norm}(t_k^+) - \dot{q}_{\rm norm}(t_k^-)) \geq 0$ (kinetic consistency).

We are now going to analyze the energetical consistency, and for that we need equivalent expressions of $T_L(t_k)$:

$$T_L(t_k) = \frac{1}{2}(\dot{q}_{\rm norm}(t_k^+) + \dot{q}_{\rm norm}(t_k^-))^T \bar{p}_{\rm n}(t_k), \tag{6.46}$$

which is the Thomson and Tait formula, or:

$$T_L(t_k) = \frac{1}{2}\dot{q}_{\rm norm}(t_k^-)^T(\mathscr{E}_{\rm nn} - I)^T G(q)^{-1}(\mathscr{E}_{\rm nn} + I)\dot{q}_{\rm norm}(t_k^-), \tag{6.47}$$

or, using the symmetry of $G(q)$[11]:

$$T_L(t_k) = \frac{1}{2}\dot{q}_{\rm norm}(t_k^-)^T(\mathscr{E}_{\rm nn}^T G(q)^{-1}\mathscr{E}_{\rm nn} - G(q)^{-1})\dot{q}_{\rm norm}(t_k^-), \tag{6.48}$$

or, following [455] and with $\xi(t_k) = \dot{q}_{\rm norm}(t_k^+) + \mathscr{E}_{\rm nn}\dot{q}_{\rm norm}(t_k^-)$:

$$T_L(t_k) = \frac{1}{2}\bar{p}_{\rm n}(t_k)^T(2\xi(t_k) - (I - \mathscr{E}_{\rm nn})G(q)\bar{p}_{\rm n}(t_k)). \tag{6.49}$$

[11] $x^T\mathscr{E}_{\rm nn}^T G(q)^{-1}x = x^T(\mathscr{E}_{\rm nn}^T G(q)^{-1})^T x = x^T G(q)^{-1}\mathscr{E}_{\rm nn}x$ for any vector $x \in \mathbb{R}^p$.

We then have several results stating conditions such that the generalized impact law is energetically consistent.

Proposition 6.3 *Suppose that* $-(\mathscr{E}_{\rm nn}-I)^T G(q)^{-1}(\mathscr{E}_{\rm nn}+I)$ *or* $-(\mathscr{E}_{\rm nn}^T G(q)^{-1}\mathscr{E}_{\rm nn}-G(q))^{-1}$ *are copositive matrices. Then* $T_L(t_k)\leq 0$. *If they are strictly copositive then* $T_L(t_k)<0$ *for any nonzero pre-impact velocity.*

Proof Due to the impact conditions one has $\dot{q}_{\rm norm}(t_k^-)\leq 0$, in other words the p dimensional vector $-\dot{q}_{\rm norm}(t^-)$ belongs to $\mathbb{R}^p_+$. From the definition of copositivity the results follow.

Proposition 6.4 *Suppose that* $\mathscr{E}_{\rm nn}=G(q)\mathscr{E}_{\rm nn}^T G(q)^{-1}$ *and* $G(q)$ *is positive definite. Then a necessary and sufficient condition for* $T_L(t)\leq 0$ *for any vector* $\dot{q}_{\rm norm}(t_k^-)$ *is that* $|\lambda_{\max}(\mathscr{E}_{\rm nn})|\leq 1$.

Proof From (6.48) we have $T_L(t_k)\leq 0$ for any $\dot{q}_{\rm norm}(t_k^-)$ if and only if $\mathscr{E}_{\rm nn}^T G(q)^{-1}\mathscr{E}_{\rm nn}\leq G(q)^{-1}$. Let $G^{\frac{1}{2}}(q)$ be the symmetric positive definite square root of $G(q)$. This inequality is equivalent to $G^{\frac{1}{2}}(q)\mathscr{E}_{\rm nn}^T G(q)^{-1}\mathscr{E}_{\rm nn}G^{\frac{1}{2}}(q)\leq I$, using Proposition 8.1.2 xi) and xiii) in [136]. Let us denote $B(q)=G^{\frac{1}{2}}(q)\mathscr{E}_{\rm nn}^T G^{-\frac{1}{2}}(q)$. By the assumption of the proposition we have $G^{-\frac{1}{2}}(q)\mathscr{E}_{\rm nn}G^{\frac{1}{2}}(q)=G^{\frac{1}{2}}(q)\mathscr{E}_{\rm nn}^T G^{-\frac{1}{2}}(q)$ so $B(q)=B^T(q)$, and since $B^T(q)=G^{-\frac{1}{2}}(q)\mathscr{E}_{\rm nn}G^{\frac{1}{2}}(q)$ we obtain $B^2(q)\leq I$. Using [136, Lemma 8.4.1] it follows that equivalently $\lambda_{\max}(B^2(q))\leq 1$, because $B^2(q)=B(q)B^T(q)$ is positive semi definite and symmetric. Now we have that $B^2(q)=G^{\frac{1}{2}}(q)(\mathscr{E}_{\rm nn}^T)^2G^{-\frac{1}{2}}(q)$, and since it is a symmetric matrix one obtains $B^2(q)=G^{-\frac{1}{2}}(q)\mathscr{E}_{\rm nn}^2G^{\frac{1}{2}}(q)$. Therefore $B^2(q)$ and $\mathscr{E}_{\rm nn}^2$ are similar matrices so they have the same eigenvalues [700, Proposition 1, p. 152]. Therefore $\lambda_{\max}(\mathscr{E}_{\rm nn}^2(q))\leq 1$. Since the eigenvalues of $\mathscr{E}_{\rm nn}^2$ are the squares of those of $\mathscr{E}_{\rm nn}$ the result follows.

The condition imposed in Proposition 6.4 holds if for instance $\mathscr{E}_{\rm nn}=\text{diag}(e_{\rm n})$. In fact $\mathscr{E}_{\rm nn}=G(q)\mathscr{E}_{\rm nn}^T G(q)^{-1}$ is equivalent to $G(q)^{-1}\mathscr{E}_{\rm nn}=\mathscr{E}_{\rm nn}^T G(q)^{-1}$, which allows us to rewrite (6.48) as:

$$T_L(t)=\frac{1}{2}\dot{q}_{\rm norm}(t_k^-)^T[(\mathscr{E}_{\rm nn}^T\mathscr{E}_{\rm nn}-I)G(q)^{-1}]\dot{q}_{\rm norm}(t_k^-) \tag{6.50}$$

Proposition 6.5 *Let* $G(q)>0$. *Then* $T_L(t_k)\leq 0$ *if* $\sigma_{\max}(\mathscr{E}_{\rm nn})\leq\frac{1}{\sqrt{\lambda_{\max}(G(q))\lambda_{\max}(G^{-1}(q))}}$, *which implies that* $\sigma_{\max}(\mathscr{E}_{\rm nn})\leq 1$.

Proof The proof begins similarly to the proof of Proposition 6.4, and we obtain that $T_L(t)\leq 0\Leftrightarrow B(q)B^T(q)\leq I$ with $B(q)=G^{\frac{1}{2}}(q)\mathscr{E}_{\rm nn}^T G^{-\frac{1}{2}}(q)$. By [136, Lemma 8.4.1] one has equivalently $\lambda_{\max}(B(q)B^T(q))=\sigma^2_{\max}(B(q))\leq 1$. From [136, Corollary 9.6.5] one has $\sigma_{\max}(B(q))\leq\sigma_{\max}(G^{\frac{1}{2}}(q))\sigma_{\max}(G^{-\frac{1}{2}}(q))\sigma_{\max}(\mathscr{E}_{\rm nn})$. Therefore $\sigma_{\max}(G^{\frac{1}{2}}(q))\sigma_{\max}(G^{-\frac{1}{2}}(q))\sigma_{\max}(\mathscr{E}_{\rm nn})\leq 1$ implies that $\sigma^2_{\max}(B(q))\leq 1$. From the symmetry and positive definiteness of $G(q)$ and of its square root,

one has $\sigma_{\max}(G^{\frac{1}{2}}(q)) = \sqrt{\lambda_{\max}(G(q))}$, so the result follows. For the last statement notice that $I = G^{-\frac{1}{2}}(q)G^{\frac{1}{2}}(q)$ so again from [136, Corollary 9.6.5] $1 \leq \sigma_{\max}(G^{\frac{1}{2}}(q))\sigma_{\max}(G^{-\frac{1}{2}}(q)) = \sqrt{\lambda_{\max}(G(q))\lambda_{\max}(G^{-1}(q))}$.

Remark 6.6 Propositions 6.4 and 6.5 state in a correct way Proposition 1 in [228], which wrongly asserts that $|\lambda_{\max}(\mathscr{E}_{\rm nn})| \leq 1$ is a sufficient condition for $T_L(t) \leq 0$ under symmetry of $\mathscr{E}_{\rm nn}$. The energy consistency of an extended frictionless Moreau's law with $\mathscr{E}_{\rm nn} = \text{diag}(e_{{\rm n},i})$ is analysed in [730, Sect. 7.1] [455], starting from the Thomson and Tait formula (6.46), or from (6.47), or from (6.49). Actually one may use Propositions 7.1 and 7.2 in [730] to analyze (6.50). The condition of Proposition 6.4 is quite close to the commuting conditions of [730, p. 159]. Finally let us remind that in the case Poisson coefficients are used (kinetic impact law) one obtains similar expressions for the loss of kinetic energy (see Eq.(43) in [458]). The quadratic forms in (6.47)–(6.49) therefore possess a general interest for both kinematic and kinetic impact laws. As shown in [210, Sect. 3.1.1], when $\mathscr{E}_{\rm nn} = \text{diag}(e_{\rm n})$ for some CoR $e_{\rm n} \in [0, 1]$, then we recover Moreau's impact law, which is always kinematically and kinetically consistent from Proposition 6.2.

Remark 6.7 From (6.42), the quasi-velocity $\dot{q}_{\rm tan}(\cdot)$ is conserved at frictionless impacts. The physical meaning of $\dot{q}_{\rm tan}(\cdot)$ may change from a system to another one. For a particle hitting a plane, this is the tangent velocity at the contact point $v_{\rm t}$, for a chain of aligned beads this is the velocity of the gravity center of the chain.

Remark 6.8 Starting from (6.42) and (6.44), and assuming kinematic, kinetic and energetic consistencies hold, we can rewrite equivalently the restitution law as:

$$\left\{\begin{array}{c} 0 \leq \dot{q}_{\rm norm}(t_k^+) + \mathscr{E}_{\rm nn}\dot{q}_{\rm norm}(t_k^-) \perp \bar{p}_{\rm n}(t_k) \geq 0 \\ \\ \Longleftrightarrow \ (\text{if } D_{\rm n}(q(t_k)) \succ 0) \\ \\ 0 \leq D_{\rm n}(q(t_k))^{-1}\bar{p}_{\rm n}(t_k) + (I + \mathscr{E}_{\rm nn}\dot{q}_{\rm norm}(t_k^-) \perp \bar{p}_{\rm n}(t_k) \geq 0, \end{array}\right. \tag{6.51}$$

which is quite similar to (5.67) and (5.68), (5.70). Going a step further:

$$D_{\rm n}(q(t_k))[\dot{q}_{\rm norm}(t_k^+) - \dot{q}_{\rm norm}(t_k^-)] \in -N_{\mathbb{R}_+^{m_u}}(\dot{q}_{\rm norm}(t_k^+) + \mathscr{E}_{\rm nn}\dot{q}_{\rm norm}(t_k^-)). \tag{6.52}$$

Let us end this section with Carnot's Theorem:

Theorem 6.1 (Carnot's Theorem) *A frictionless impact after which persistent contact is established, is always accompanied by a kinetic energy loss.*

Proof From (6.42) and (6.46), and taking $\dot{q}_{\rm norm}(t_k^+) = 0$ (i.e. without loss of generality, we suppose that m contacts are established), it follows that $T_L(t_k) = -\frac{1}{2}\dot{q}_{\rm norm}(t_k^-)^T D_{\rm n}(q(t_k))\dot{q}_{\rm norm}(t_k^-) \leq 0$, and this holds even if the constraints are not independent, because $D_{\rm n}(q) \succeq 0$.[12]

[12] Recall however that we assume that $M(q) \succ 0$, for the basic definition of the vectors $\mathbf{n}_{q,i}$.

A geometric interpretation of Carnot's Theorem is given in [569]. It is noteworthy that Theorem 6.1 is stated without chosing any particular restitution mapping.

6.2.5 *Restitution Law with Tangential Effects*

The impact dynamics is in this case equal to:

$$\begin{cases} \dot{q}_{\text{norm}}(t^+) - \dot{q}_{\text{norm}}(t^-) = \mathbf{n}_q^T M(q)\mathbf{n}_q \ \bar{p}_n(t) + \mathbf{n}_q^T H_{\text{T}}(q) \ p_{\text{t}} \\ \dot{q}_{\text{tan}}(t^+) - \dot{q}_{\text{tan}}(t^-) = \mathbf{t}_q^T H_{\text{T}}(q) \ p_{\text{t}}. \end{cases} \tag{6.53}$$

We saw in Sect. 4.3 that tangential effects may be introduced in kinematic restitution laws in three ways: tangential restitution, Coulomb's law at the impulse level, and a mixture of both. Tangential restitution can be readily inserted in (6.45), by defining non null restitution submatrices $\mathscr{E}_{\text{nt}}$, $\mathscr{E}_{\text{tn}}$ and $\mathscr{E}_{\text{tt}}$. For the sake of briefness we present next an extension of the model studied in Sects. 4.3.1.1, 4.3.1.2 and 4.3.1.5, with $\tilde{v}_{\text{t}}(t_k) = v_{\text{t}}(t_k^+) + e_{\text{t}} v_{\text{t}}(t_k^-)$, and $\mathscr{E}_{\text{nt}} = 0$, $\mathscr{E}_{\text{tn}} = 0$ and $\mathscr{E}_{\text{tt}} = 0$ in the restitutiuon matrix $\mathscr{E}$: the tangential restitution submatrix $\mathscr{E}_{\text{tt}}$ is introduced thorugh Coulomb's law. We restrict ourselves to planar friction at each contact point i, and write Coulomb's law at the impulse level as:

$$p_{\text{t},i} \in -\mu_i \, p_{\text{n},i} \ \text{sgn}(v_{\text{t},i}(t_k^+) + e_{\text{t},i} v_{\text{t},i}(t_k^-)) \tag{6.54}$$

for some tangential CoRs $e_{\text{t,i}}$, $1 \leq i \leq m_u'$, which copies (4.69). In the examples studied in Sects. 4.3.1.1, 4.3.1.2 and 4.3.1.5, we proved that it was always possible to compute a unique $v_{\text{t}}(t_k^+)$ when this tangential model is used (see (4.73) and (4.83)). In the general case the mere existence issue if more complex. Inserting (6.54) into (6.42) we find:

$$\begin{cases} -(I + \mathscr{E}_{\text{nn}})\dot{q}_{\text{norm}}(t_k^-) \in G(q)\bar{p}_{\text{n}}(t_k) - \mathbf{n}_q^T H_{\text{t}}(q)[\bar{\mu}][\bar{p}_{\text{n}}(t_k)]\text{Sgn}(v_{\text{t}}(t_k^+) + \mathscr{E}_{\text{tt}} v_{\text{t}}(t_k^-)) \\ \qquad\qquad\qquad\qquad\qquad\qquad \overbrace{\qquad\qquad\qquad\qquad}^{\triangleq \tilde{V}_{\text{t}}(t_k)} \\ \dot{q}_{\text{tan}}(t_k^+) - \dot{q}_{\text{tan}}(t_k^-) \in -\mathbf{t}_q^T H_{\text{t}}(q)[\bar{\mu}][\bar{p}_{\text{n}}(t_k)]\text{Sgn}(\underbrace{v_{\text{t}}(t_k^+) + \mathscr{E}_{\text{tt}} v_{\text{t}}(t_k^-)}) \end{cases} \tag{6.55}$$

with: $[\bar{\mu}] = \text{diag}\left(\frac{\mu_i}{||\nabla f_i(q)||_{M^{-1}}}\right) \in \mathbb{R}^{m_u' \times m_u'}$, $[\bar{p}_n] = \text{diag}(\bar{p}_{\text{n},i})$, $\mathscr{E}_{\text{tt}} = \text{diag}(e_{\text{t},i})$, $v_{\text{t}} = H_{\text{t}}(q)^T \Xi^T(q) v$ (v is in (6.23)), $\text{Sgn}(\tilde{V}_{\text{t}}(t_k)) = (\text{sgn}(\tilde{v}_{\text{t},1}(k), \ldots, \text{sgn}(\tilde{v}_{\text{t},m_u'}(t_k))^T$. The unknowns of the generalized equation (6.55) are the m_u' impulses $\bar{p}_{\text{n},i}$, and the $n - m_u'$ quasi-velocities $\dot{q}_{\text{tan},i}(t_k^+)$, with the constraints $\bar{p}_{\text{n},i} \geq 0$ and $\dot{q}_{\text{norm}}(t_k^+) = -\mathscr{E}_{\text{nn}}\dot{q}_{\text{norm}}(t_k^-)$. The first inclusion in (6.55) may be used to find an extension of (4.90), and we may look for a generalized Lemma 4.1 for the kinetic constraint satisfaction. It may be rewritten equivalently as[13]:

[13] Notice that we recover here a matrix $G^{\mu}(q, v_{\text{t}}(t_k^+))$ which has the same structure as $D^{\mu}(q)$ in (5.158).

$$\overbrace{(G(q)-\mathbf{n}_q^T H_{\mathrm{t}}(q)[\bar{\mu}][\xi_i])}^{\triangleq G^{\mu}(q,v_{\mathrm{t}}(t_k^+))}\bar{p}_{\mathrm{n}}(t_k)\ni -(I+\mathscr{E}_{\mathrm{nn}})\dot{q}_{\mathrm{norm}}(t_k^-) \tag{6.56}$$

with $[\xi_i]=\mathrm{diag}(\xi_i)$ and $\xi_i\in\mathrm{sgn}(\tilde{v}_{\mathrm{t},i}(t_k))$. We can use Theorem 5.8 to guarantee that for small enough friction $\mu_i\leq\mu_{\max}(q)$, $1\leq i\leq m_u$, then $G^{\mu}(q,v_{\mathrm{t}}(t_k^+))\succ 0$ for any frictional mode (i.e. any $\xi_i\in[\text{-}1,1]$), and then insert the found value of $\bar{p}_{\mathrm{n}}(t_k)$ in the second inclusion of (6.55). This gives rise to the program: Given the data $q(t_k)$ and $\dot{q}(t_k^-)$, and the parameters $\mathscr{E}_{\mathrm{nn}}$, $\mathscr{E}_{\mathrm{tt}}$, find $\dot{q}(t_k^+)$ such that:

$$\begin{aligned}&\mathbf{t}_q^T M(q)\dot{q}(t_k^+)=\dot{q}_{\tan}(t_k^-)+\mathbf{t}_q^T H_{\mathrm{t}}(q)[\bar{\mu}](G^{\mu}(q,H_{\mathrm{t}}(q)^T\dot{q}(t_k^+)))^{-1}(I+\mathscr{E}_{\mathrm{nn}})\dot{q}_{\mathrm{norm}}(t_k^-)\xi\\&\text{with: }\nabla f(q)^T\dot{q}(t_k^+)=-\mathscr{E}_{\mathrm{nn}}\dot{q}_{\mathrm{norm}}(t_k^-)\\&\qquad\xi\in\mathrm{Sgn}(H_{\mathrm{t}}(q)^T\dot{q}(t_k^+)+\mathscr{E}_{\mathrm{tt}}v_{\mathrm{t}}(t_k^-))\Leftrightarrow H_{\mathrm{t}}(q)^T\dot{q}(t_k^+)\in-\mathscr{E}_{\mathrm{tt}}v_{\mathrm{t}}(t_k^-)+N_{[-1,1]}(\xi)\end{aligned} \tag{6.57}$$

where we recall that $v_{\mathrm{t}}=H_{\mathrm{t}}(q)^T\dot{q}$ from the local kinematics, and we denoted $q(t_k)$ as q. If this program possesses a solution $\dot{q}(t_k^+)$, then the impact problem with friction is solvable with kinematic and kinetic constraints satisfied. See Sect. 4.3.1.5 for an example, with normal/tangential couplings. The generalized equation is rather tricky since it can hardly be put in a canonical form $0\in F(x)+N_K(x)$, with $F(\cdot)$ continuous and $K=[\text{-}1,1]^{m_u'}$, so that [385, Corollary 2.2.5] may be applied.[14] This fact is not surprizing because the original problem in (6.55) is already nonlinear in its unknowns, due to the products between $\bar{p}_{\mathrm{n}}(t_k)$ and $\mathrm{Sgn}(\tilde{V}_{\mathrm{t}}(t_k))$.

Let us pass now to the energetical behavior of this impact law with friction, assuming that we could find at least one solution to (6.57). Choosing one of these solutions provides us with $\tilde{V}_{\mathrm{t}}(t_k)$ and most importantly with a selection $\xi\in\mathrm{Sgn}(\tilde{V}_{\mathrm{t}}(t_k))$. Extension of (6.46) through (6.49) is:

$$\begin{aligned}T_L(t_k)&=\tfrac{1}{2}\dot{q}_{\mathrm{norm}}(t_k^+)^T D_{\mathrm{n}}(q)\dot{q}_{\mathrm{norm}}(t_k^+)-\tfrac{1}{2}\dot{q}_{\mathrm{norm}}(t_k^-)^T D_{\mathrm{n}}(q)\dot{q}_{\mathrm{norm}}(t^-)\\&+\tfrac{1}{2}\dot{q}_{\tan}(t_k^+)^T D_{\mathrm{t}}(q)\dot{q}_{\tan}(t_k^+)-\tfrac{1}{2}\dot{q}_{\tan}(t_k^-)^T D_{\mathrm{t}}(q)\dot{q}_{\tan}(t_k^-)\\&=\tfrac{1}{2}(\dot{q}_{\mathrm{norm}}(t_k^+)+\dot{q}_{\mathrm{norm}}(t^-))^T D_{\mathrm{n}}(q)(\dot{q}_{\mathrm{norm}}(t_k^+)-\dot{q}_{\mathrm{norm}}(t_k^-))\\&+\tfrac{1}{2}(\dot{q}_{\tan}(t_k^+)+\dot{q}_{\tan}(t_k^-))^T D_{\mathrm{t}}(q)(\dot{q}_{\tan}(t_k^+)-\dot{q}_{\tan}(t_k^-))\\&=\tfrac{1}{2}(\dot{q}_{\mathrm{norm}}(t_k^+)+\dot{q}_{\mathrm{norm}}(t_k^-))^T[\bar{p}_{\mathrm{n}}(t_k)+G(q)\mathbf{n}_q^T H_{\mathrm{t}}(q)p_{\mathrm{t}}(t_k)]\\&+\tfrac{1}{2}(\dot{q}_{\tan}(t_k^+)+\dot{q}_{\tan}(t_k^-))^T D_{\mathrm{t}}(q)\mathbf{t}_q^T H_{\mathrm{t}}(q)p_{\mathrm{t}}(t_k).\end{aligned} \tag{6.58}$$

[14] **Corollary 6.1** *[385, Corollary 2.2.5] Let $K\subseteq\mathbb{R}^n$ be compact convex, and $F:K\to\mathbb{R}^n$ be continuous. Then, the set of solutions to the generalized equation $0\in F(x)+N_K(x)$ is nonempty and compact.*

We assume that the problem (6.55) has been solved for at least one $\bar{p}_{\mathrm{n}}(t_k)$ and one $\dot{q}(t_k^+)$. Then after few manipulations we obtain:

$$\begin{aligned} T_L(t_k) = &-\tfrac{1}{2}\dot{q}_{\mathrm{norm}}(t_k^-)^T \overbrace{(I-\mathscr{E}_{\mathrm{nn}})^T M(q,\mu,v_{\mathrm{t}}(t_k^+))(I+\mathscr{E}_{\mathrm{nn}})}^{\triangleq \bar{M}(q,\mu,v_{\mathrm{t}})} \dot{q}_{\mathrm{norm}}(t_k^-) \\ &+\dot{q}_{\mathrm{tan}}(t_k^-)^T D_{\mathrm{t}}(q)\mathbf{t}_q^T H_{\mathrm{t}}(q)[\bar{\mu}][\xi] G^{\mu}(q,v_{\mathrm{t}}(t_k^+)))^{-1}(I+\mathscr{E}_{\mathrm{nn}})\dot{q}_{\mathrm{norm}}(t_k^-) \\ &+\tfrac{1}{2}\dot{q}_{\mathrm{norm}}(t_k^-)^T K(q,\mu,v_{\mathrm{tt}}(t_k^+))\dot{q}_{\mathrm{norm}}(t_k^-) \end{aligned} \tag{6.59}$$

with $M(q,\mu,v_{\mathrm{t}}) \triangleq G^{\mu}(q,v_{\mathrm{t}})^{-1} - G(q)\mathbf{n}_q^T H_{\mathrm{t}}(q)[\bar{\mu}][\xi] G^{\mu}(q,v_{\mathrm{t}})^{-1}$ and $K(q,\mu,v_{\mathrm{t}}(t_k^+)) \triangleq (I+\mathscr{E}_{\mathrm{nn}})^T G^{\mu}(q,v_{\mathrm{t}}(t_k^+))^{-T}[\bar{\mu}][\xi] H_{\mathrm{t}}(q)^T \mathbf{t}_q D_{\mathrm{t}}(q)\mathbf{t}_q^T H_{\mathrm{t}}(q)[\bar{\mu}][\xi]$ $G^{\mu}(q,v_{\mathrm{t}}(t_k^+))^{-1}(I+\mathscr{E}_{\mathrm{nn}})$. Let us investigate the positive definiteness of the matrix $\bar{M}(M(q,\mu,v_{\mathrm{t}})$.

Proposition 6.6 *[210] Assume that $G(q) \succ 0$. Then:*

1. *If $||G(q)^{-1}||_2||\mathbf{n}_q^T H_{\mathrm{t}}(q)||_2||[\bar{\mu}]||_2 < 1$, one has $G^{\mu}(q,v_{\mathrm{t}}(t_k^+))^{-1} \succ 0$.*
2. *If $||G^{\mu}(q,v_{\mathrm{t}}(t_k^+))||_2||G^{\mu}(q,v_{\mathrm{t}}(t_k^+))^{-1}||_2||G(q)||_2||\mathbf{n}_q^T H_{\mathrm{t}}(q)||_2||[\bar{\mu}]||_2 < 1$ is satisfied, then $M(q,\mu,v_{\mathrm{t}})) \succ 0$.*
3. *If $||\mathscr{E}_{\mathrm{nn}}||_2(1+2||\mathscr{E}_{\mathrm{nn}}||_2) < \frac{1}{||M(q,\mu,v_{\mathrm{t}})||_2} \frac{1}{\left|\left|\left(\frac{M(q,\mu,v_{\mathrm{t}}))+M^T(q,\mu,v_{\mathrm{t}}))}{2}\right)^{-1}\right|\right|_2}$ is satisfied, then $\bar{M}(q,\mu,v_{\mathrm{t}}) \succ 0$.*

Proof (1) $G(q)$ is symmetric positive definite. Applying Theorem 5.8 with $N = G(q)$ and $D = G(q) - \mathbf{n}_q^T H_{\mathrm{T}}(q)[\bar{\mu}][\xi]$ one finds that the inequality in 1 guarantees that $G(q) - \mathbf{n}_q^T H_{\mathrm{T}}(q)[\bar{\mu}][\xi]$ is positive definite. Then this matrix has a positive definite inverse which is $G^{\mu}(q,v_{\mathrm{t}})$. (2) The proof follows from Corollary 5.2, with $M = G^{\mu}(q,v_{\mathrm{t}})^{-1}$, $B = I - G(q)\mathbf{n}_q^T H_{\mathrm{t}}(q)[\bar{\mu}][\xi]$ and $A = M(q,\mu,v_{\mathrm{t}})$. Applying Proposition 9.3.5 in [136] to upper-bound $||G(q)\mathbf{n}_q^T H_{\mathrm{t}}(q)[\bar{\mu}][\xi]||_2$ by the product of norms, the result follows. (3) One has $(I-\mathscr{E}_{\mathrm{nn}})^T M(q,\mu,v_{\mathrm{t}})(I+\mathscr{E}_{\mathrm{nn}}) = M(q,\mu,v_{\mathrm{t}}) + H(q,\mu,e_{\mathrm{n,i}})$, with $H(q,\mu,e_{\mathrm{n,i}}) = -\mathscr{E}_{\mathrm{nn}}^T M(q,\mu,v_{\mathrm{t}})\mathscr{E}_{\mathrm{nn}} - \mathscr{E}_{\mathrm{nn}}^T M(q,\mu,v_{\mathrm{t}}) + M(q,\mu,v_{\mathrm{t}})\mathscr{E}_{\mathrm{nn}}$. Consider Theorem 5.8, with $M = M(q,\mu,v_{\mathrm{t}})$ and $A = M(q,\mu,v_{\mathrm{t}}) + H(q,\mu,e_{\mathrm{n,i}})$. Using Proposition 9.3.5 in [136] and the triangular inequality of norms one finds $||H(q,\mu,e_{\mathrm{n,i}})||_2 \leq ||\mathscr{E}_{\mathrm{nn}}||_2^2||M(q,\mu,v_{\mathrm{t}})||_2 + 2||\mathscr{E}_{\mathrm{nn}}||_2||M(q,\mu,v_{\mathrm{t}})||_2$. Thus it suffices that

$$\left|\left|\left(\frac{M(q,\mu,v_{\mathrm{t}})+M^T(q,\mu,v_{\mathrm{t}})}{2}\right)^{-1}\right|\right|_2 (||\mathscr{E}_{\mathrm{nn}}||_2^2||M(q,\mu,v_{\mathrm{t}})||_2 + 2||\mathscr{E}_{\mathrm{nn}}||_2||M(q,\mu,v_{\mathrm{t}})||_2) < 1$$

and the result follows.

From (6.59) the following holds:

$$T_L(t_k) \leq -\tfrac{1}{2}\lambda_{\min}(\bar{M}(q,\mu,v_{\mathrm{t}}))||\dot{q}_{\mathrm{norm}}(t_k^-)||^2 + \tfrac{1}{2}\lambda_{\max}(K(q,\mu,v_{\mathrm{t}}))||\dot{q}_{\mathrm{norm}}(t_k^-)||^2$$
$$+||D_{\mathrm{t}}(q)\mathbf{t}_q^T H_{\mathrm{t}}(q)||_2||[\bar{\mu}]||_2||I+\mathscr{E}_{\mathrm{nn}}||_2||\dot{q}_{\mathrm{norm}}(t_k^-)||\ ||\dot{q}_{\mathrm{tan}}(t_k^-)|| \tag{6.60}$$

Theorem 6.2 *[210] Provided that*

$$(i)\ \lambda_{\min}(\bar{M}(q,\mu,v_{\mathrm{t}}(t_k^+))) > \lambda_{\max}(K(q,\mu_i,v_{\mathrm{t}}(t_k^+)))$$
$$(ii)\ \frac{||\dot{q}_{\mathrm{norm}}(t_k^-)||}{||\dot{q}_{\mathrm{tan}}(t_k^-)||} \geq 2\frac{||D_{\mathrm{t}}(q)\mathbf{t}_q^T H_{\mathrm{t}}(q)||_2||[\bar{\mu}]||_2||I+\mathscr{E}_{\mathrm{nn}}||_2}{\lambda_{\min}(\bar{M}(q,\mu,v_{\mathrm{t}}(t_k^+)))-\lambda_{\max}(K(q,\mu,v_{\mathrm{t}}(t_k^+)))}, \tag{6.61}$$

one has $T_L(t_k) \leq 0$.

Proof Follows directly from (6.60).

Example 6.2 Let us illustrate the above developments on the simplest case of a planar particle hitting a line. The horizontal position is x, the vertical one (normal to the line) is y. One has $\dot{q}_{\mathrm{norm}} = \sqrt{m}\dot{y}$, $\dot{q}_{\mathrm{tan}} = \sqrt{m}\dot{x}$, $\bar{p}_{\mathrm{n}} = \frac{1}{\sqrt{m}}p_{\mathrm{n}}$, $G^{\mu}(q,v_{\mathrm{t}}) = 1$, $M(q,\mu) = 1, \bar{M}(q,\mu) = 1-e_{\mathrm{n}}^2, K(q,\mu_i,x(t_k^+)) = \mu^2(1+e_{\mathrm{n}})^2, D_{\mathrm{t}} = 1, \mathbf{t}_q^T D_{\mathrm{t}}\mathbf{t}_q = \frac{1}{m}, \mathbf{t}_q^T H_{\mathrm{t}}(q) = \frac{1}{\sqrt{m}}, G(q) = 1, \bar{p}_{\mathrm{n}} = -(1+e_{\mathrm{n}})\dot{q}_{\mathrm{norm}}(t_k^-), \ddot{q}_{\mathrm{norm}} = \bar{p}_{\mathrm{n}}, \ddot{q}_{\mathrm{tan}} = \frac{1}{\sqrt{m}}p_{\mathrm{t}}$, $\dot{q}_{\mathrm{tan}}(t^+) - \dot{q}_{\mathrm{tan}}(t_k^-) = \frac{1}{\sqrt{m}}(1+e_{\mathrm{n}})\dot{q}_{\mathrm{norm}}(t_k^-)\bar{\mu}\xi$, with $\xi \in \mathrm{sgn}(\dot{x}(t_k^+) + e_{\mathrm{t}}\dot{x}(t^-))$. The conditions of the Theorems imply that $e_{\mathrm{n}} \leq 1$, while the kinematic admissibility implies that $e_{\mathrm{n}} \geq 0$. The direct application of Theorem 6.2 gives:

$$(i)\ 1-e_{\mathrm{n}} > \mu^2(1+e_{\mathrm{n}})$$
$$(ii)\ \frac{|\dot{y}(t_k^-)|}{|\dot{x}(t_k^-)|} \geq \frac{2\mu}{1-e_{\mathrm{n}}-\mu^2(1+e_{\mathrm{n}})}. \tag{6.62}$$

Notice that condition (i) implies that $e_{\mathrm{n}} < 1$. If $e_{\mathrm{n}} = 0$ then $\mu < 1$ and $\frac{|\dot{y}(t_k^-)|}{|\dot{x}(t_k^-)|} \geq \frac{2\mu}{1-\mu^2}$. If $e_{\mathrm{n}} = 1$ only the frictionless case is admitted, because in that case $\bar{M}(q,\mu,v_{\mathrm{t}}) = 0$, and we have excluded this case from the beginning.

Remark 6.9 The major drawback of the generalized kinematic impact law, is that in most cases one has to identify the parameters for a given collision, i.e. for a given set of initial data and mechanical parameters: this is mainly due to the lack of information on contact flexibility in the model, which hampers to predict wave effects inside the multibody system. The LZB law introduced in Sect. 6.3 is from this point of view, much better. A possible way to enhance the generalized kinematic law, could be to use the information about the postimpact pattern, which is sometimes available (see Fig. 5.5 where two general patterns appear, see also [621, Fig. 1] for a two-ball system hitting a wall). Another drawback is related with its insertion in a

time-stepping algorithm for simulation: does it have to be used only in event-driven integrators?

6.2.6 Tangential Restitution

Motivated by the models described in Sects. 4.3.1, 4.3.2 and 4.3.3, where a tangential restitution coefficient is discussed *vs.* Coulomb's friction at the impulse level, we may introduce a generalized restitution as follows. We may impose $\bar{p}_{\rm n} \in -N_{V_{\rm n}(q)}(\Gamma_{\rm n}(\dot{q}_{\rm norm}(t^+) + \Lambda_{\rm n}\dot{q}_{\rm norm}(t^-)))$ and $p_{\rm t} \in -N_{V_{\rm t(q)}}(\Gamma_{\rm t}(\dot{q}_{\rm tan}(t^+) + \Lambda_{\rm t}\dot{q}_{\rm tan}(t^-)))$, for some matrices $\Lambda_{\rm n}$, $\Lambda_{\rm t}$, $\Gamma_{\rm n}$, $\Gamma_{\rm t}$, and convex sets $V_{\rm n}(q)$ and $V_{\rm t}(q)$. Inserting this into (6.53) one obtains the generalized equation:

$$v(t^+) - v(t^-) \in -\bar{G}(q) \begin{pmatrix} N_{V_{\rm n}(q)}(\Gamma_{\rm n}(\dot{q}_{\rm norm}(t^+) + \Lambda_{\rm n}\dot{q}_{\rm norm}(t^-))) \\ N_{V_{\rm t(q)}}(\Gamma_{\rm t}(\dot{q}_{\rm tan}(t^+) + \Lambda_{\rm t}\dot{q}_{\rm tan}(t^-))) \end{pmatrix}. \tag{6.63}$$

Defining the convex set $W(q) \stackrel{\Delta}{=} V_{\rm n}(q) \times V_{\rm t}(q)$ and Λ =diag$(\Lambda_{\rm n}, \Lambda_{\rm t})$, Γ =diag $(\Gamma_{\rm n}, \Gamma_{\rm t})$, we get :

$$v(t^+) - v(t^-) \in -\bar{G}(q)\, N_{W(q)}(\Gamma(v(t^+) + \Lambda v(t^-))), \tag{6.64}$$

with $\bar{G}(q) = \begin{pmatrix} G(q) & \mathbf{n}_q^T H_{\rm T}(q) \\ 0 & \mathbf{t}_q^T H_{\rm T}(q) \end{pmatrix}$. Existence and uniqueness of a solution $v(t^+)$ to the generalized equation in (6.64) depend on the matrices $\bar{G}(q)$, Γ, Λ, and on the convex sets $V_{\rm n}(q)$ and $V_{\rm t}(q)$. Suppose that there exists a symmetric positive definite matrix P such that $P\bar{G}(q) = \Gamma^T$, and let us denote R its symmetric square root $R^2 = P$. Then, using Convex Analysis tools (which we already used a lot throughout this book) we get:

$$v(t^+) = -\Lambda v(t^-) + R^{-1}\text{proj}[\bar{W}(q);\, R(\Lambda + I)v(t^-)] \tag{6.65}$$

with $\bar{W}(q) = \{x | \bar{G}^T Rx \in W(q)\}$ a convex set.

6.2.7 Comments

The generalized restitution law (6.44) and (6.45) has been studied in detail when applied on the planar rocking block and chains of aligned balls, in [228] (see Sect. 6.3.2.2). The domains where the entries of $\mathscr{E}_{\rm nn}$ have to lie in order for kinematic, kinetic and energetic consistencies to hold, are summarized in [228, Table 1]

in several cases: free rocking with or without sliding, half-rocking. It is also shown that the three consistency constraints plus the pre-impact velocity, do not define a unique set of CoRs (entries of $\mathscr{E}_{\rm nn}$) in general, or that some of the CoRs are admissible while >1. As noted by Moreau [900], adding a tangential CoR within a generalized framework, is more a trick than the result of deep modeling. The normalized Delassus's matrix is the matrix of *kinetic angles* between the constraints. More precisely, the kinetic angle between two constraints is defined as

$$\theta_{ij}(q) = \pi - \arccos \frac{\nabla f_i(q)^T M^{-1}(q) \nabla f_j(q)}{\sqrt{\nabla f_i(q)^T M^{-1}(q) \nabla f_i(q)} \sqrt{\nabla f_j(q)^T M^{-1}(q) \nabla f_j(q)}}. \quad (6.66)$$

Kinetic angles are quantities that reflect the couplings between the inertial and the geometrical properties of the system with unilateral constraints. It readily follows that $\mathbf{n}_q^T M(q) \mathbf{n}_q = [\cos(\pi - \theta_{ij})] = -[\cos(\theta_{ij})]$. In particular $\theta_{ii} = \pi$ and the diagonal entries are $-\cos(\theta_{ii}) = 1$. Kinetic angles play a major role in continuity of solutions w.r.t. initial data (see Sect. 5.2.4). Obviously they also play a major role in multiple impacts, for if constraints are pairwise orthogonal, then the Delassus's matrix is diagonal and collisions are decoupled. We based the definition of the generalized impact law in (6.44) and (6.45) on geometrical arguments, starting from the normal vectors $\mathbf{n}_{q,i}$ in (6.22), which have the interpretation of normals to the constraint boundary where $f_i(q) = 0$ in the kinetic metric. This is the only little piece of differential geometry in this book. For readers who like to swim in geometrical waters, let us refer to [305, 568, 980, 981]. The tangential restitution operator in Sect. 6.2.6 is strongly inspired from Frémond [414, 415] and close results have also been stated in [455, 730]. Sufficient conditions about energetic consistency may be found in [228, Sect. 3.2]. The most general restitution matrix (with tangential $\mathscr{E}_{\rm tt}$ and normal/tangential couplings $\mathscr{E}_{\rm nt}$ and $\mathscr{E}_{\rm tn}$) may be seen as an extension of Brach's approach in (4.103), formulated in a Lagrange dynamics context instead of Newton-Euler's dynamics. Interestingly enough, it happens in some applications like rockfalls [169] that a diagonal restitution matrix like in (4.103) is not sufficient: couplings have to be considered [169, Eq. (4)], and stochastic model of the CoRs is needed [168, 169, 170].

6.3 Energetic-CoR Multiple-Impact Law

We describe in this section an extension of the Darboux-Keller's shock dynamics, which applies to multiple impacts. Like for the Darboux-Keller's approach, the positions are assumed to be constant during the impact, and the dynamics is integrated with respect to the contact force impulse. This was introduced in [749, 750, 753, 1327], and is named the LZB impact dynamics.

6.3.1 Presentation of the LZB Impact Dynamics

The LZB approach yields an extension of the Darboux-Keller's impact dynamics, in case of multiple contacts/impacts. Thus basic assumptions are constant position q, and negligible forces (other than the impact forces) during the shock. It uses a bistiffness model as in Fig. 4.6a. We recall that this model is a crude approximation of the force/indentation law for elasto-plastic rate-independent materials, because it does not limit the contact force, and it dissipates energy even for very low pre-impact velocity (hence, for very low impact velocities which are below the minimum plastification velocity, a monostiffness model should be used). Moreover, it models dissipation during the expansion phase, while plasticification occurs during the compression phase (loading), see Sect. 4.2.1. An improvement is proposed in [929, Sect. 4.2.7] which we do not describe here.

Let F_j be the contact force at contact point j, and δ_j the normal indentation (whence $\dot{\delta}_j = \nabla f_j(q)^T \dot{q}$). During the compression (loading) phase, $F_{c,j} = k_j (\delta_{c,j})^{\eta_j}$, and during the expansion (unloading) phase, $F_{e,j} = F_{\max,j} \left(\frac{\delta_{e,j} - \delta_{r,j}}{\delta_{c,j} - \delta_{r,j}} \right)^{\eta_j}$. The corresponding works are given by $W_{c,j} = \int_0^{\delta_{c,j}} F_{c,j}(\delta_{c,j}) d\delta_{c,j} = \frac{1}{1+\eta_j} k_j (\delta_{c,j})^{\eta_j+1}$, and $W_{e,j} = \int_{\delta_{c,j}}^{\delta_{r,j}} F_{e,j}(\delta_{e,j}) d\delta_{e,j} = -\frac{1}{1+\eta_j} k (\delta_{c,j})^{\eta_j} (\delta_{c,j} - \delta_{r,j})$. Using the energetical CoR $e_{\star,j}$ as defined in (4.159), we infer that $\delta_{r,j} = \delta_{c,j}(1 - e_{\star,j}^2)$, which relates the CoR and the residual indentation. Notice that $\delta_{c,j}$ is the maximum compression indentation, so it is not a parameter of the impact dynamics, it is computed by integration of the collision dynamics. Few manipulations show that we also have $e_{\star,j}^2 = \frac{\delta_{c,j} - \delta_{r,j}}{\delta_{c,j}} = \left(\frac{k_{c,j}}{k_{e,j}} \right)^{\frac{1}{\eta_j}}$,[15] where $k_{c,j} = k_j$ is the stiffness during compression, $k_{e,j} = k_{c,j} \left(\frac{\delta_{c,j}}{\delta_{c,j} - \delta_{r,j}} \right)^{\eta_j}$ is the stiffness during expansion. According to the bistiffness model, the work done by the contact force during compression, is entirely converted into elastic potential energy stored in the bodies. Thus, the potential energy at the "instant" p_j during compression is $E_j(p_j) = \int_0^{p_j} \dot{\delta}_j(p_j) dp_j$, $0 \le p_j \le p_{c,j}$, where $p_{c,j}$ corresponds to maximal compression.[16] Then the residual potential energy during the expansion phase, is $E_j(p_j) = \int_0^{p_{c,j}} \dot{\delta}_j(p_j) dp_j + \frac{1}{e_{\star,j}^2} \int_{p_{c,j}}^{p_i} \dot{\delta}_j(p_j) dp_j = W_{c,j} + \frac{1}{e_{\star,j}^2} \int_{p_{c,j}}^{p_i} \dot{\delta}_j(p_j) dp_j$, $p_{c,j} \le p_j \le p_{f,j}$, where $p_{f,j}$ is the normal contact force impulse at the end of the expansion phase. The proof of this is given in [750, Sect. 3 (b)].

The normal contact force satisfies during the compression phase $\frac{dF_j}{dt} = \frac{dF_j}{dp_j} \frac{dp_j}{dt} = F_j \frac{dF_j}{dp_j}$, hence using that $\frac{dF_j}{dt} = \eta_j k_j (\delta_j)^{\eta_j - 1} \nabla f_j(q)^T \dot{q}$, we deduce that $F_j^{\frac{1}{\eta_j}} dF_j = \eta_j k_j^{\frac{1}{\eta_j}} \nabla f_j(q)^T \dot{q} \, dp_j$. We finally obtain $F_j(p_j) = \left((\eta_j + 1) \int_0^{p_j} k_j^{\frac{1}{\eta_j}} \nabla f_j(q)^T \dot{q} \, dp_j \right)^{\frac{\eta_j}{1+\eta_j}}$. We remind that these calculations are possible because it is assumed that the position

[15] This is consistent with what is stated in Sect. 4.2.1.2.

[16] We should denote $p_{\mathrm{n},j}$ to be consistent with the notations adopted elsewhere in the book.

q is constant, $q = q(0)$. One can then deduce that the ratio of two normal impulses at contact points j and i is given by $\frac{dp_j}{dp_i} = \frac{(\eta_j+1)^{\frac{\eta_j}{\eta_j+1}} k_j^{\frac{1}{\eta_j+1}} \left(\int_0^{p_j} \nabla f_j(q)^T \dot{q}\, dp_j\right)^{\frac{\eta_j}{\eta_j+1}}}{(\eta_i+1)^{\frac{\eta_i}{\eta_i+1}} k_i^{\frac{1}{\eta_i+1}} \left(\int_0^{p_i} \nabla f_i(q)^T \dot{q}\, dp_i)\right)^{\frac{\eta_i}{\eta_i+1}}}$. Noting that the potential energy $E_j(p_j)$ at contact point j equals $\int_0^{p_j} \nabla f_j(q)^T \dot{q}\, dp_j$, we can rewrite the impulse ratio as $\frac{dp_j}{dp_i} = \frac{(\eta_j+1)^{\frac{\eta_j}{\eta_j+1}} k_j^{\frac{1}{\eta_j+1}} (E_j(p_j))^{\frac{\eta_j}{\eta_j+1}}}{(\eta_i+1)^{\frac{\eta_i}{\eta_i+1}} k_i^{\frac{1}{\eta_i+1}} (E_i(p_i))^{\frac{\eta_i}{\eta_i+1}}}$. The next question is whether this continues to hold during the whole compression/expansion cycle. The answer is yes, as shown in [750, Sect. 3(d)].

In general there may be either a precompression at the contact point j, or a *repeated collision*: a first collision starts (compression, then expansion), but a second compression phase starts again before the expansion phase terminates (i.e., before the contact j opens), followed by an expansion phase. Suppose that the force/indentation relationship remains unchanged during repeated impacts, as depicted in Fig. 6.6. It is possible to prove the following, during a repeated impact at contact j:

$$E_j(p) = \begin{cases} E_0 + \int_0^{p_j} \dot{\delta}_j(p_j)\, dp_j & \text{if } Q \in \widehat{OM_{c,1}} \\ E_{M_{c,1}} + \frac{1}{e_{\star,j}^2} \int_{p_{M_{c,1}}}^{p_j} \dot{\delta}_j(p_j)\, dp_j & \text{if } Q \in \widehat{M_{c,1}R} \\ E_R + \int_{p_R}^{p_j} \dot{\delta}_j(p_j)\, dp_j & \text{if } Q \in \widehat{RM_{c,2}} \\ E_{M_{c,2}} + \frac{1}{e_{\star,j}^2} \int_{p_{M_{c,2}}}^{p_j} \dot{\delta}_j(p_j)\, dp_j & \text{if } Q \in \widehat{M_{c,2}B}, \end{cases} \tag{6.67}$$

where the cycle is as in Fig. 6.6 and Q is a generic point on the force/indentation curve corresponding to time p_j. The quantities E_0, $E_{M_{c,1}}$, E_R and $E_{M_{c,2}}$ are the residual potential energies at the points O, $M_{c,1}$, R and $M_{c,2}$, respectively. If the initial contact force at contact j is $F_{0,j}$ with indentation $\delta_{0,j}$, then, the initial potential energy is $E_{0,j} = \int_0^{\delta_{0,j}} \lambda_{c,j}(\delta_j) d\delta_j = \frac{(F_{0,j})^{\frac{\eta_j+1}{\eta_j}}}{(\eta_j+1) k_j^{\frac{1}{\eta_j+1}}}$. From the above expression of $F_j(p_j)$, we infer that $F_j(p_j) = (1+\eta_j)^{\frac{\eta_j}{\eta_j+1}} k_j^{\frac{1}{\eta_j+1}} \left(\frac{(F_{0,j})^{\frac{\eta_j+1}{\eta_j}}}{(\eta_j+1) k_j^{\frac{1}{\eta_j+1}}} + \int_0^{p_j} \dot{\delta}_j(p_j) dp_j \right)^{\frac{\eta_j}{\eta_j+1}}$, where one sees from (6.67) that the term between brackets is the potential enery $E_j(p_j)$. After some calculations the contact force during the expansion phase satisfies $F_{e,j} dF_{e,j} = \eta_j F_{\max,j} \left(\frac{\delta_j - \delta_{r,j}}{\delta_{c,j} - \delta_{r,j}}\right)^{\eta_j - 1} \frac{\dot{\delta}_j}{\delta_{c,j} - \delta_{r,j}} dp_j$, and using that $\delta_{c,j} - \delta_{r,j} = e_{\star,j}^2 \delta_{c,j}$, one finds $(F_{e,j})^{\frac{1}{\eta_j}} dF_{e,j} = \eta_j (F_{e,j})^{\frac{1}{\eta_j}} \frac{\dot{\delta}_j}{e_{\star,j}^2 \delta_{c,j}} dp_j$. At the end of the compression phase we have $F_{c,j} = k_j (\delta_{c,j})^{\eta^j}$, hence $(F_{e,j})^{\frac{1}{\eta_j}} dF_{e,j} = \frac{1}{e_{\star,j}^2} \eta_j (k_j)^{\frac{1}{\eta_j}} \dot{\delta}_j dp_j$. At the beginning of the expansion phase, we have $p_j = p_{c,j}$ and $\dot{\delta}_j = 0$, and $F_j(p_{c,j}) = (1+\eta_j)^{\frac{\eta_j}{1+\eta_j}} k_j^{\frac{1}{\eta_j}+1} (E_j(p_{c,j}))^{\frac{\eta_j}{\eta_j+1}}$. Integrating one obtains $(F_{e,j}(p_j))^{\frac{\eta_j+1}{\eta_j}} = (\eta_j + 1) k_j^{\frac{1}{\eta_j+1}} E_j(p_j)$. Thus the contact force during expansion at the impulse instant p_j is

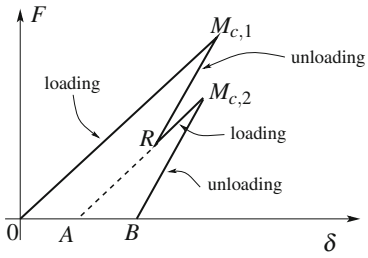

Fig. 6.6 A repeated impact (linear elasticity: $\eta = 1$)

given by $F_{e,j} = (1+\eta_j)^{\frac{\eta_j}{1+\eta_j}} k_j^{\frac{1}{1+\eta_j}} (E_j(p_j))^{\frac{\eta_j}{1+\eta_j}}$. This is the same expression as for the compression phase.
We therefore deduce that the ratios of the normal contact forces impulses at contact points j and i, are given generically by the *distributing rule*:

$$\Gamma_{ji} = \frac{dp_j}{dp_i} = \frac{(1+\eta_j)^{\frac{\eta_j}{\eta_j+1}} k_j^{\frac{1}{1+\eta_j}} E_j^{\frac{\eta_j}{1+\eta_j}}}{(1+\eta_i)^{\frac{\eta_i}{\eta_i+1}} k_i^{\frac{1}{1+\eta_i}} E_i^{\frac{\eta_i}{1+\eta_i}}}. \tag{6.68}$$

It follows that if the elasticity constants $\eta_j = \eta - i = \eta$, then Γ_{ij} does depend only on the stiffness ratio $\gamma_{ji} = \frac{k_j}{k_i}$, not on the absolute values of the stiffnesses. This is coherent with what we already noticed in Sect. 6.1.3 on a particular case. It is interesting to see now that this is not true if the elasticity coefficients are not identical. The multiple impact terminates when all the potential energy that has been stored during the compression phases, is entirely released or dissipated and all contacts open, that is $E_j(p_{f,j}) = 0$ and $\dot{\delta}_j(p_{f,j}) \geq 0$ for all j that participate into the collision. The LZB impact dynamics is summarized as follows:

- Contact parameters $e_{\star,j}$, η_j, $1 \leq j \leq m$, γ_{ij}, precompression potential energies $E_{0,j}$ and indentations $\delta_{0,j}$.
- Darboux-Keller's dynamics:

$$\boldsymbol{M}(q)\frac{d\dot{\boldsymbol{q}}}{dp_i} = \nabla f(q)\boldsymbol{\Gamma}, \tag{6.69}$$

  with contact i being the primary contact.
- Ratio $\Gamma_{ji} = \dfrac{dp_j}{dp_i}$ of the normal impulse increment at contact j to that at the primary contact i:

$$\Gamma_{ji} = \frac{(1+\eta_j)^{\eta_j/(\eta_j+1)}}{(1+\eta_i)^{\eta_i/(\eta_i+1)}} \frac{k_j^{1/(1+\eta_j)}}{k_i^{1/(1+\eta_i)}} \frac{E_j^{\eta_j/(\eta_j+1)}}{E_i^{\eta_i/(\eta_i+1)}}. \tag{6.70}$$

and $\Gamma = (\Gamma_{1i}, \Gamma_{2i}, .., \Gamma_{i-1,i}, 1, \Gamma_{i+1,i}, \ldots, \Gamma_{mi})^T$.

- Potential energy E_j:

$$E_j(p_j) = \int_0^{p_j} \dot{\delta}_j(p_j) dp_j, \text{ if } 0 \leq p_j \leq p_{c,j}, \tag{6.71}$$

$$E_j(p_j) = W_{c,j} + \frac{1}{e_{\star,j}^2} \int_{p_{c,j}}^{p_j} \dot{\delta}_j(p_j) dp_j, \text{ if } p_j^c \leq p_j \leq p_{f,j}, \tag{6.72}$$

with $\dot{\delta}_j = \nabla f_j(q)^T \dot{q}$, $p_{c,j}$ is the impulse at the end of the compression phase ($\dot{\delta}_j(p_{c,j}) = 0$), and $p_{f,j}$ is the terminal impulse.

- Impact termination condition:

$$E_j = 0, \ \dot{\delta}_j \leq 0, \text{ for all } j = 1, 2, \ldots, m. \tag{6.73}$$

where m is the number of impacting points.

The primary impulse p_i has to be chosen properly, for in particular it should not vanish, and may be changed during the collision integration. Its choice for the numerical integration of the LZB impact dynamics, is explained in [753], and in [929, Algorithm 3, page 90]. A numerical algorithm is detailed in [753] which explains how the LZB impact dynamics may be integrated. See also [929, Sects. 4.2, 4.3] for a very detailed presentation of the LZB dynamics integration and its insertion in an event-driven algorithm. The case with friction is detailed in [752]. Possible numerical instability due to the elasticity coefficients η_j that make the LZB dynamics stiff, is studied in [929, § 4.2.9].

6.3.2 Applications and Validations

The LZB model has been validated through numerous comparisons with experimental data.

6.3.2.1 Chains of Aligned Beads

Probably the most fundamental microscopic property of granular materials is irreversible energy dissipation in the course of interaction (collision) between particles [56]. A correct modeling of the dissipation at impacts (and also outside impacts during persistent contact phases of motion), and a correct numerical algorithm for simulation, are therefore of utmost importance in granular matter. Chains of balls are a first, simple instance of granular mechanical systems. Numerical results with the LZB model have been compared to experimental results obtained on various types of chains of aligned balls [387, 625, 838, 915, 1059], in [749, 753, 928, 929, 1331]. Some of them have been presented in Figs. 6.1 and 6.2a, b. The comparisons concern

not only the postimpact velocities and kinetic energy, but also and most importantly the waves that travel through the chains, maximum impact force and force pulse amplitude for monodisperse as well as tapered and stepped chains [753, 928, 929]. They prove that the LZB model encapsulates the main phenomena (nonlinear waves) which are responsible for the multiple impact. As we said above, this is due to the fact that the LZB model contains the information on stiffness ratios between the contact points. A complete exposition of the event-driven codes used to simulate the chains, is made in [929]. *The LZB model for multiple impacts may be the very first instance where it is proved experimentally that the energetic CoR supersedes the kinematic and the kinetic CoRs*.

Further Reading: Newton's cradle and chains of balls are apparently simple, almost toy-systems, however thet have received a lot of attention since a long time, especially in the Physics teachers literature. Since the appearance of Granular Matter as a scientific field, and the discoveries of their great complexity from the point of view of nonlinear waves transmission, they serve as an example of one-dimensional granular material. We do not survey all the results about chains of aligned beads in this book. Let us mention that the discovery of nonlinear solitary waves in monodisperse chains (identical balls) is due to Nesterenko [924], and justified experimentally in [306]. Since then nonlinear waves have been studied in several types of chains, varying the radii (hence the masses) of the balls, the contact interaction potentials, and the curve of the chain [145, 245, 529, 608, 609, 610, 613, 772, 956, 1012, 1086] to cite a few.

6.3.2.2 Rocking Block

We consider the system in Fig. 6.7a, which has two unilateral constraints (provided the base line is assumed to be concave) when $y \leq \frac{\sqrt{l^2+L^2}}{2}$: $f_1(q) = y - \frac{l}{2}\cos(\theta) + \frac{L}{2}\sin(\theta) \geq 0$, and $f_2(q) = y - \frac{l}{2}\cos(\theta) - \frac{L}{2}\sin(\theta) \geq 0$. It is interesting to notice that the admissible domain Φ which depicted in Fig. 6.7b, is not convex. Assuming that the dynamical effects of the block on the base are negligible, the dynamics of the block with Coulomb friction is given by

$$\left\{\begin{array}{l} m\ddot{x}(t) = \lambda_{\mathrm{t},1}(t) + \lambda_{\mathrm{t},2}(t) \\ m\ddot{y}(t) = \lambda_{\mathrm{n},1}(t) + \lambda_{\mathrm{n},2}(t) - mg \\ I_G\ddot{\theta}(t) = \lambda_{\mathrm{n},1}(t)\left(\frac{l}{2}\sin(\theta(t)) + \frac{L}{2}\cos(\theta(t))\right) + \lambda_{\mathrm{n},2}(t)\left(\frac{l}{2}\sin(\theta(t)) - \frac{L}{2}\cos(\theta(t))\right) \\ \qquad + \left(\frac{l}{2}\cos(\theta(t)) - \frac{L}{2}\sin(\theta(t))\right)\lambda_{\mathrm{t},1} + \left(\frac{l}{2}\cos(\theta(t)) + \frac{L}{2}\sin(\theta(t))\right)\lambda_{\mathrm{t},2} \\ \\ \qquad 0 \leq \lambda_{\mathrm{n}}(t) \perp f(q(t)) \geq 0 \\ \qquad \lambda_{\mathrm{t},i}(t) \in -\mu_i\lambda_{\mathrm{n},i}(t)\ \mathrm{sgn}(v_{\mathrm{t},i}(t) - v_b(t)), i = 1, 2, \end{array}\right. \tag{6.74}$$

where $v_b(t) = \dot{x}_b(t)$ is the base horizontal velocity, $\mu_i > 0$ is the friction coefficient at contact i, and $v_{\mathrm{t},i}$ is the tangential velocity at the point i, i.e. $v_{\mathrm{t},1} = \dot{x} + \left(\frac{l}{2}\cos(\theta) - \frac{L}{2}\sin(\theta)\right)\dot{\theta}$ at B and $v_{\mathrm{t},2} = \dot{x} + \left(\frac{l}{2}\cos(\theta) + \frac{L}{2}\sin(\theta)\right)\dot{\theta}$ at A (from which $v_{\mathrm{t},1} = v_{\mathrm{t},2}$ when $\theta = 0$). With $q = (x, y, \theta)^T$, one can identify M, F_{ext}, $\nabla f(q)$ and $H_{\mathrm{t}}(q)$ in (5.1) from (6.74).

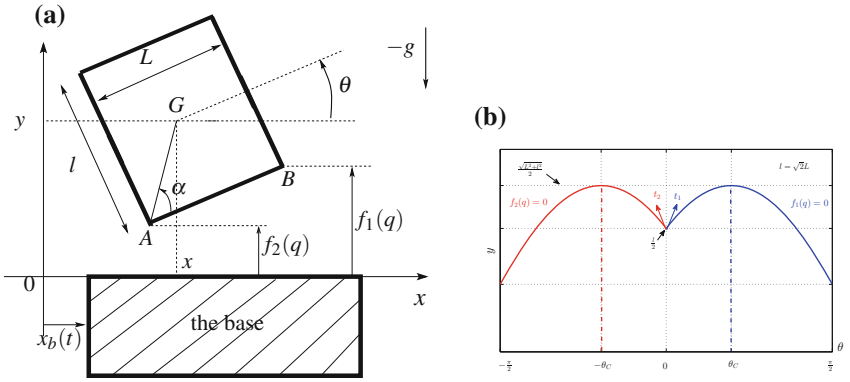

Fig. 6.7 The rocking block. **a** The system. **b** Admissible domain (taken from [1318])

The contact LCP is $0 \leq \lambda_{\mathrm{n}} \perp D_{\mathrm{nn}}(\theta)\lambda_{\mathrm{n}} + \nabla f(\theta)^T M^{-1} H_{\mathrm{t}}(\theta)\lambda_{\mathrm{t}} + B(\theta, \dot{\theta}) \geq 0$ with $D_{\mathrm{nn}}(\theta) = \begin{pmatrix} \frac{1}{m} + \frac{1}{4I_G}(l\sin(\theta) + L\cos(\theta))^2 & \frac{1}{m} + \frac{1}{4I_G}(l^2\sin^2(\theta) - L^2\cos^2(\theta)) \\ \frac{1}{m} + \frac{1}{4I_G}(l^2\sin^2(\theta) - L^2\cos^2(\theta)) & \frac{1}{m} + \frac{1}{4I_G}(l\sin(\theta) - L\cos(\theta))^2 \end{pmatrix}$ and $B(\theta, \dot{\theta}) = \begin{pmatrix} -g + \frac{1}{2}\dot{\theta}^2(l\cos(\theta) - L\sin(\theta)) \\ -g + \frac{1}{2}\dot{\theta}^2(l\cos(\theta) + L\sin(\theta)) \end{pmatrix}$. The Delassus' matrix $D_{\mathrm{nn}}(\theta) \succ 0$ except at $\theta = \pm\frac{\pi}{2}$.

Remark 6.10 (Kinetic Angles) The kinetic angle θ_{12} between the two constraints is given by:

$$\theta_{12} = \pi - \arccos\left(\frac{l^2 - 2L^2}{l^2 + 4L^2}\right) \tag{6.75}$$

at $\theta = 0$. Denoting the aspect ratio as $a \stackrel{\Delta}{=} l/L$ we may rewrite it as $\theta_{12} = \pi - \arccos\left((a^2 - 2)/(a^2 + 4)\right)$: there is a one-to-one correspondence between a and θ_{12}. It satisfies $\theta_{12} = \pi/2$ if $l = \sqrt{2}L$, $0 < \theta_{12} < \pi/2$ if $0 < l < \sqrt{2}L$ (flat block), and $\pi > \theta_{12} > \pi/2$ if $l > \sqrt{2}L$ (slender block). When a varies from 0 (infinitely flat block with infinite width L) to $+\infty$ (infinitely slender block with infinite height l) then θ_{12} varies from $\pi/4$ to π. The fact that $\theta_{12} \in [\pi/4, \pi]$ means that one expects that the block/ground system possesses a rich dynamics, and may serve as a nice example of multiple impact with friction. The interest of studying the block dynamics as a function of the kinetic angle between the two boundaries at $\theta = 0$, is that it allows us to determine that a block is not of the slender type just if $l > L$. As shown in [1318] using the LZB model with friction, the dispersion factor $d \stackrel{\Delta}{=} \frac{\dot{y}_A(t_k^+)}{\dot{y}_B(t_k^-)}$ displays a particular $V-$shaped as a function of θ_{12} (equivalently of a) and for varying friction [1318, Figs. 6, 7, 12], and there exists a critical kinetic angle at which d is minimum, which is independent of the CoR [1318, Fig. 10], see Fig. 6.8b.

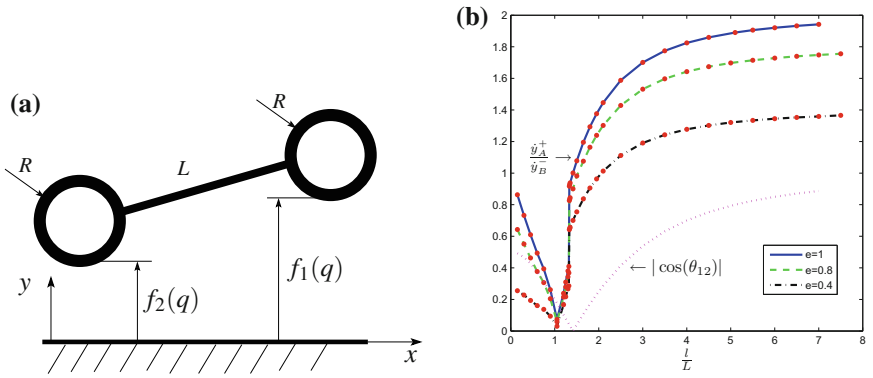

Fig. 6.8 The dimer, and rocking block's critical aspect ratio. **a** The bouncing dimer. **b** Critical kinetic angle for the rocking block's energy dispersion (taken from [1318])

Remark 6.11 (Kinetic Angles (continued)) A system that is close to the classical rocking block, is the bouncing dimer studied in [357, 1327] and depicted in Fig. 6.8a. The dimer is made of two identical spheres with radius R connected by a rigid rod with length L. Using the same notations as for the block, the two unilateral constraints for the dimer are $f_1(q) = y + (L/2 + R)\sin(\theta) - R \geq 0$ and $f_2(q) = y - (L/2 + R)\sin(\theta) - R \geq 0$. Some calculations yield that the kinetic angle between the two constraints at $\theta = 0$ (double impact) and with all masses equal to 1 for simplicity, is given by $\theta_{12} = \pi - \arccos\left((1/3 - \alpha)/(1/3 + \alpha)\right)$ with $\alpha = (1+2a)^2/(16a^2/5 + 1/3 + 2(1+2a)^2)$, $a = R/L$. The flatest dimer has $L = +\infty$, and the less flat one has $L = 0$ (the two balls are stuck together). The two kinetic angle values that correspond to these extreme cases are $\theta_{12} = \pi - \arccos(-1/8) \approx 1.445$ rad and $\theta_{12} = \pi - \arccos(-1/29) \approx 1.536$ rad, which are both slightly smaller than $\pi/2 \approx 1.571$ rad. This means that the dimer and the block, despite their apparent similarity, possess different dynamical behaviors in the sense that the dimer kinetic angle varies little and never exceeds $\pi/2$ (the dimer is always flat), while the block kinetic angle may vary much more.

The LZB model applied to the block/anvil system for rocking, onset of rocking, with harmonic base excitations, is validated in [1319] with thorough comparisons between numerical simulations and the experimental data obtained on blue granite stone blocks reported in [987, 988].[17] The masses of the blocks are estimated from their dimensions and density, and are given by 503, 228, 120, 245 kg, demonstrating the scope of the experiments. The overturning phenomenon is also analysed in [1319].

[17] All the experimental data used for the comparisons with numerical data presented in [1319] have been made available to the authors by Dr F. Pena from Instituto di Ingenieria, UNAM, Mexico.

It is noteworthy that the parameters (equivalent width and length, CoRs) have been fitted from the free-rocking experimental data, and then used without modification for the other comparisons with an excited base (onset of rocking).

Further Reading, Comments and Perspectives: The rocking block dynamics has been studied since a long time in the Earthquake Engineering literature, because of its interest in better understanding buildings dynamics under seismic excitation, see e.g. [19, 41, 42, 379, 543, 747, 1010, 1017, 1131]. The restitution law that is widely used is $\dot{\theta}(t_k^+) = e_\theta \dot{\theta}(t_k^-)$ for some CoR e_θ. This seems to be an *ad hoc* restitution law, however this is not quite the case. The link between $\mathscr{E}$ in (6.44) and (6.45) and e_θ as well as local tangential restitution is made in [228]. It is found that in case of rocking motion (the block rotates around A, hits the ground at B without rebound, then rotates around B, hits the ground at A without rebound, etc), we have $\mathscr{E} = \begin{pmatrix} 0 & -e_\theta & 0 \\ -e_\theta & 0 & 0 \\ 0 & 0 & e_\theta \end{pmatrix}$. Therefore, *the angular velocity CoR is interpreted via the generalized restitution law, as a tangential CoR for* $\dot{q}_{\tan}$. Moreover, let $v_{\mathrm{t},i}(t_k^+) = e_{\mathrm{t}} v_{\mathrm{t},i}(t_k^+)$, $i = 1, 2$ at A and B, where e_{t} is the local tangential CoR. Then it can be shown that $e_{\mathrm{t}} = -e_{\mathrm{t},3} = -e_{\mathrm{n},1} + e_{\mathrm{n},21}$ [228, Sect. 6]. It follows that if one imposes in addition that there is no slip at the impacting point, then $e_{\mathrm{t}} = 0$, while no rebound at the impacting point implies $e_{\mathrm{n},1} = 0$. We infer that necessarily $\mathscr{E} = 0$. It is also proved in [228, Sect. 3.6] that Coulomb's friction (at the impulse level) with $\tilde{v}_{\mathrm{t}}(t_k) = v_{\mathrm{t}}(t_k^+)$ in (4.69) and a diagonal $\mathscr{E}_{\mathrm{nn}}$, cannot model rocking motion: off-diagonal terms in $\mathscr{E}_{\mathrm{nn}}$ and tangential restitution CoR are needed. It is nevertheless noteworthy that such impact law cannot model very finely the real block motion. In practice, one observes usually rebounds at both A and B even during a rocking global motion, and slip/stick phases.

Some experiments in [987, 988] show the existence of non-negligible three-dimensional effects, due to body vibrations and torsion. This proves the need to go beyond planar systems. The study of three-dimensional rocking blocks with flexibilities is an interesting topic for future investigations. The rocking block system involves *line/line impact* (or *plane/plane impact* in the thee-dimensional case), for which the two-point contact model is a crude approximation (implying in particular the estimation of an equivalent width which does not necessarily match with the geometrical width). Line/line impacts modeling is investigated in [1330].

6.3.2.3 Other Experimental Validations of the LZB Model

The LZB model has been further validated with careful comparisons between experimental and numerical data, in [1248, 1249] (three-dimensional bouncing dimer), [1327] (two-dimensional bouncing dimer), a disk-ball system [748, 1321].

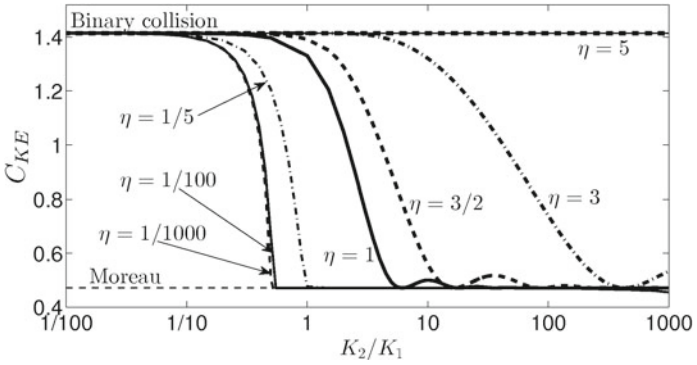

Fig. 6.9 Relation C_{KE} - k_2/k_1 for different values of η: Moreau, binary collisions, LZB (taken from [929, Fig. 6.12])

6.3.3 Comparison of Different Multiple Impact Mappings

A thorough comparison between Moreau's law, the binary collision model, and the LZB approach, is made on the monodisperse three-ball chain in [929, Chap. 6]. The comparisons are made by varying elasticity coefficients, masses, and stiffnesses ratio, with the "usual" initial conditions (the first bead hits the other two, in contact and at rest). We present in Fig. 6.9 the kinetic energy dispersion variable C_{KE} defined in (5.72) in Chap. 5, as a function of the stiffness ratio $\frac{k_2}{k_1}$ and the elasticity coefficient η ($\eta = 1$ for linear elasticity, $\eta = \frac{3}{2}$ for Hertz' elasticity, etc). This figure shows that the energy dispersion varies significantly with η and $\frac{k_2}{k_1}$, and that Moreau's law applies for low C_{KE} index[18] (i.e. high dispersion, "large" $\frac{k_2}{k_1}$ and "small" η), while the binary collision applies to high C_{KE} index (i.e. low dispersion, "small" $\frac{k_2}{k_1}$ and "large" η). Such analysis would deserve an extension to more general chains, in order to determine validity areas for Moreau/Newton, binary collision, Pfeiffer-Glocker/Poisson approaches. Once again it is clear that the great advantage of the LZB approach is that it encapsulates information on the stiffness ratio. The domains of validity of the Moreau's or binary collisions laws, depend in turn on the form of the waves created by the collision between the first and the second balls, which varies depending on η_j [529, 1086]. Let us mention an interesting comparative analysis between visco-elastic models (see Chap. 2), binary collisions approach, bistiffness model and elasto-plastic approaches (see Sect. 4.2.1), when applied on the three-ball system in [354].

[18] In agreement with Proposition 5.17 which states that Moreau's law minimizes C_{KE}.

6.4 Further Reading

6.4.1 Kinetic Restitution (Poisson)

Pfeiffer and Glocker introduced a generalization of Poisson's impact law in [1001]. It consists of solving a two-stage LCP at each contact point. Let us illustrate it on a simple case of two aligned balls hitting a wall. A crucial assumption is that the maximum compression times at each contact/impact point, are equal (see [929, Sect. 3.1.2] for detailed calculations on a 3-ball chain, showing the necessity of this assumption). This may be the main and less realistic hypothesis of this approach, because in most cases maximum compression times do not match, and there may even exist repeated impacts. Let us apply the method to the case of a chain of two balls, that strikes a rigid wall (i.e., take $N = 2$ in Fig. 6.1). Roughly, the problem is solved by constructing two LCPs, one for the end of the compression phase ($t = t_c$), the second one for the end of the expansion phase ($t = t_f$). Coefficients $e_{\mathrm{p},1}$ and $e_{\mathrm{p},2}$ are associated with each contact. The LCPs at each contact, $i = 1, 2$, are as follows:

- At $t = t_c$:

$$\left\{\begin{array}{l} p_i(t)\,\dot{f}_i(q(t)) = 0 \\ \dot{f}_i(q(t)) \geq 0 \\ p_i(t) \geq 0 \end{array}\right. \tag{6.76}$$

- At $t = t_f$:

$$\left\{\begin{array}{l} p_i(t_f) - p_i(t_c) - e_{\mathrm{p},i}\,p_i(t_c) \geq 0 \\ \dot{f}_i(q(t_f)) \geq 0 \\ \{p_i(t_f) - p_i(t_c) - e_{\mathrm{p},i}\,p_i(t_c)\}\,\dot{f}_i(q(t_f)) = 0 \end{array}\right. \tag{6.77}$$

where $f_1(q) = q_1 - q_2$ and $f_2(q) = q_2$ are the two unilateral constraints. Introducing the impact dynamics (we use the same initial data and masses as above) $\dot{q}_1(t_c) + 1 = p_1(t_c), \dot{q}_2(t_c) = -p_1(t_c) + p_2(t_c), \dot{q}_1(t_f) - \dot{q}_1(t_c) = p_1(t_f) - p_1(t_c), \dot{q}_2(t_f) - \dot{q}_2(t_c) = -p_1(t_f) + p_1(t_c) + p_2(t_f) - p_2(t_c)$, one therefore gets four LCPs (two for each contact)

$$\left\{\begin{array}{l} p_1(t_c)(\dot{q}_1 - \dot{q}_2)(t_c) = 0 \\ (\dot{q}_1 - \dot{q}_2)(t_c) \geq 0 \\ p_1(t_c) \geq 0 \end{array}\right. , \left\{\begin{array}{l} p_2(t_c)\dot{q}_2(t_c) = 0 \\ \dot{q}_2(t_c) \geq 0 \\ p_2(t_c) \geq 0 \end{array}\right. \tag{6.78}$$

$$\begin{array}{l} \left\{\begin{array}{l} p_1(t_f) - p_1(t_c) - e_{\mathrm{p},1}\,p_1(t_c) \geq 0 \\ (\dot{q}_1 - \dot{q}_2)(t_f) \geq 0 \\ \{p_1(t_f) - p_1(t_c) - e_{\mathrm{p},1}\,p_1(t_c)\}(\dot{q}_1 - \dot{q}_2)(t_c) = 0 \end{array}\right. \\ \left\{\begin{array}{l} p_2(t_f) - p_2(t_c) - e_{\mathrm{p},2}\,p_2(t_c) \geq 0 \\ \dot{q}_2(t_f) \geq 0 \\ (p_2(t_f) - p_2(t_c) - e_{\mathrm{p},2}\,p_2(t_c))(\dot{q}_1 - \dot{q}_2)(t_f) = 0. \end{array}\right. \end{array} \tag{6.79}$$

If both CoR's are equal to 1, it is easily checked that there is a unique solution given by $(\dot{q}_1 - \dot{q}_2)(t_f) = 1$, $\dot{q}_2(t_f) = 0$, so that $\dot{q}_1(t_f) = 1$ and $\dot{q}_2(t_f) = 0$. The case with friction is discussed in [1000]. It is shown in [929, Fig. 3.1] that in order to fill in the whole admissible postimpact velocity domain of Fig. 5.5, it is necessary to consider CoRs $e_{\mathrm{p},i} > 1$, which may lack of physical meaning. Pfeiffer-Glocker's approach with a two-stage LCP is used in [47, 48] in a three-dimensional setting and Coulomb friction with facetized cone. A thorough analysis of the energetic consistency of Pfeiffer-Glocker's law with or without friction, is made in [456]. It has also been implemented in [1022] for ice floes simulation with an event-driven code.

6.4.2 Kinematic Restitution (Newton and Moreau)

Inspired by Frémond whose framework introduced in Sect. 4.3.4 extends to multiple shocks [266, 290, 836] [415, Chap. 8] [416, Chapitre 5], Glocker has introduced in [451, 454, 985] a restitution matrix similar to $\mathscr{E}_{\mathrm{nn}}$ in (6.45), and makes a thorough geometrical analysis of Moreau's impact law, he also extends it to re-entrant corners [454, Sect. 5.4], which are excluded from Moreau's framework which is based on finitely represented admissible domains Φ. Leine and van de Wouw [730, 732] extend Moreau's framework by formulating impact laws with friction as inclusions in normal cones to convex sets (or the reverse inclusions in subdifferentials of support functions) [730, Chap. 5]. Restitution matrices are allowed, and conditions for dissipativity are given [730, pp.159–160] which are used for stability purpose [730, Theorem 7.6]. In [1026], a kinematic restitution matrix is introduced (in a way similar to our $\mathscr{E}_{\mathrm{nn}}$ above, or to Glocker's matrix in [451, 454, 985], see also the formulations in [730] which accomodate for restitution matrices and also friction), while friction is modeled at the impulse level with a friction cone faceting procedure.

6.4.3 Other Approaches

Bowling and Rodriguez [1048] use Routh's incremental approach and energetical CoRs at each contact in a chain of aligned balls to solve the multiple impact: energy dispersion is modeled. The same authors formulate in [171, 1047] the multiple impact with friction as an optimization problem which includes kinetic and energetic constraints, starting from the maximum dissipation principle of friction, and a diagonal restitution matrix with kinematic CoRs (this may be seen as a rewriting of Moreau's rule with friction). Barjau et al. [90, 91] use a stiff unilateral compliant normal contact model, combined with a modal analysis, for frictionless redundant contacts. Bistiffness-like models are used in [91] to account for energy loss. Jia [622, 623] presents a very detailed analysis close to the one in Sect. 6.3.1, with a state-transition diagram to describe the multiple impact. Their approach is close to the one in Sect. 6.3.1: a linear bistiffness law is chosen, repeated impacts are taken

into account, and the distributing law is derived in a particular case [623, Eq. (15)]. Hurmuzlu and co-authors introduced in [268, 441, 558, 1187, 1300] a method which consists of using Routh's incremental two-dimensional approach, with so-called impulse correlation ratios (ICR), which are constants relating the impact forces impulses (the percussion $p_{\mathrm{n},i}$ at each contact i, in the sense of Definition 1.2). The ICRs permit to introduce some distance effects (or energy dispersion) in the impact dynamics. However as shown on numerical simulations in [11] and in the above distributing rule (6.68), impulse ratios are not be constant in general but could vary a lot depending on the initial data and parameters, and should therefore be fitted with experiments. Hurmuzlu and Marghitu [561] deal with planar kinematic chains with multiple contact/impact points (see also [559] for a preliminary result). Collisions are treated with Routh' incremental method (two-dimensional Darboux-Keller's dynamics), and an event-driven-like algorithm is proposed to calculate the postimpact velocity, testing all possible cases (stick-slip transitions in both directions, constraint deactivation).